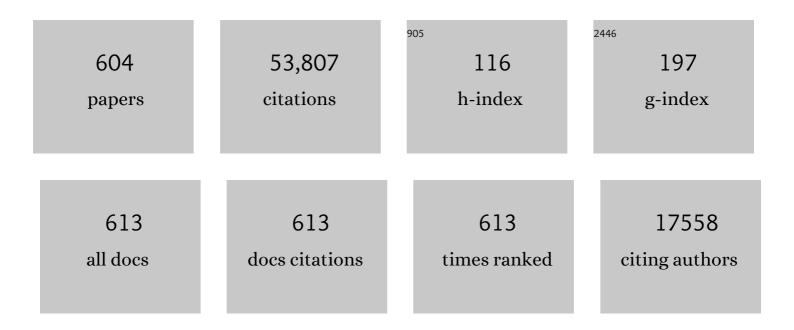


## List of Publications by Year in descending order

Source: https://exaly.com/author-pdf/10004181/publications.pdf Version: 2024-02-01



FINE

#	Article	lF	CITATIONS
1	Evidence from detrital zircons for the existence of continental crust and oceans on the Earth 4.4 Gyr ago. Nature, 2001, 409, 175-178.	13.7	1,505
2	Magmatic and Crustal Differentiation History of Granitic Rocks from Hf-O Isotopes in Zircon. Science, 2007, 315, 980-983.	6.0	1,154
3	Further Characterisation of the 91500 Zircon Crystal. Geostandards and Geoanalytical Research, 2004, 28, 9-39.	2.0	1,142
4	4.4 billion years of crustal maturation: oxygen isotope ratios of magmatic zircon. Contributions To Mineralogy and Petrology, 2005, 150, 561-580.	1.2	970
5	Prediction of crystal–melt partition coefficients from elastic moduli. Nature, 1994, 372, 452-454.	13.7	860
6	A Change in the Geodynamics of Continental Growth 3 Billion Years Ago. Science, 2012, 335, 1334-1336.	6.0	707
7	Modification and preservation of environmental signals in speleothems. Earth-Science Reviews, 2006, 75, 105-153.	4.0	669
8	Using hafnium and oxygen isotopes in zircons to unravel the record of crustal evolution. Chemical Geology, 2006, 226, 144-162.	1.4	655
9	Episodic growth of the Gondwana supercontinent from hafnium and oxygen isotopes in zircon. Nature, 2006, 439, 580-583.	13.7	640
10	UWG-2, a garnet standard for oxygen isotope ratios: Strategies for high precision and accuracy with laser heating. Geochimica Et Cosmochimica Acta, 1995, 59, 5223-5231.	1.6	632
11	Oxygen Isotopes in Zircon. Reviews in Mineralogy and Geochemistry, 2003, 53, 343-385.	2.2	626
12	MPI-DING reference glasses for in situ microanalysis: New reference values for element concentrations and isotope ratios. Geochemistry, Geophysics, Geosystems, 2006, 7, n/a-n/a.	1.0	563
13	Zircon Behaviour and the Thermal Histories of Mountain Chains. Elements, 2007, 3, 25-30.	0.5	535
14	Evolution of the continental crust. Nature, 2006, 443, 811-817.	13.7	533
15	SIMS determination of trace element partition coefficients between garnet, clinopyroxene and hydrous basaltic liquids at 2–7.5 GPa and 1080–1200°C. Lithos, 2000, 53, 165-187.	0.6	520
16	A predictive model for rare earth element partitioning between clinopyroxene and anhydrous silicate melt. Contributions To Mineralogy and Petrology, 1997, 129, 166-181.	1.2	482
17	Trace elements in speleothems as recorders of environmental change. Quaternary Science Reviews, 2009, 28, 449-468.	1.4	422
18	lsotopic evidence for rapid continental growth in an extensional accretionary orogen: The Tasmanides, eastern Australia. Earth and Planetary Science Letters, 2009, 284, 455-466.	1.8	398

#	Article	IF	CITATIONS
19	Experimental constraints on major and trace element partitioning during partial melting of eclogite. Geochimica Et Cosmochimica Acta, 2002, 66, 3109-3123.	1.6	391
20	The chemistry of zircon: Variations within and between large crystals from syenite and alkali basalt xenoliths. Geochimica Et Cosmochimica Acta, 1991, 55, 3287-3302.	1.6	382
21	A cool early Earth. Geology, 2002, 30, 351.	2.0	381
22	Partitioning of trace elements between crystals and melts. Earth and Planetary Science Letters, 2003, 210, 383-397.	1.8	357
23	Trace-element geochemistry of mantle olivine and application to mantle petrogenesis and geothermobarometry. Chemical Geology, 2010, 270, 196-215.	1.4	351
24	A dearth of intermediate melts at subduction zone volcanoes and the petrogenesis of arc andesites. Nature, 2009, 461, 1269-1273.	13.7	336
25	Heavy REE are compatible in clinopyroxene on the spinel lherzolite solidus. Earth and Planetary Science Letters, 1998, 160, 493-504.	1.8	334
26	Magmatic δ18O in 4400–3900 Ma detrital zircons: A record of the alteration and recycling of crust in the Early Archean. Earth and Planetary Science Letters, 2005, 235, 663-681.	1.8	331
27	Refining the <i>P–T</i> records of UHT crustal metamorphism. Journal of Metamorphic Geology, 2008, 26, 125-154.	1.6	294
28	An integrated microtextural and chemical approach to zircon geochronology: refining the Archaean history of the Napier Complex, east Antarctica. Contributions To Mineralogy and Petrology, 2005, 149, 57-84.	1.2	291
29	Oxygen isotope ratios and rare earth elements in 3.3 to 4.4 Ga zircons: Ion microprobe evidence for high I' 18 O continental crust and oceans in the Early Archean. Geochimica Et Cosmochimica Acta, 2001, 65, 4215-4229.	1.6	284
30	Magma heating by decompression-driven crystallization beneath andesite volcanoes. Nature, 2006, 443, 76-80.	13.7	272
31	An experimental study of amphibole stability in low-pressure granitic magmas and a revised Al-in-hornblende geobarometer. Contributions To Mineralogy and Petrology, 2016, 171, 1.	1.2	269
32	Partitioning of Sr2+ and Mg2+ into calcite under karst-analogue experimental conditions. Geochimica Et Cosmochimica Acta, 2001, 65, 47-62.	1.6	265
33	Fractionation of trace elements by subduction-zone metamorphism — effect of convergent-margin thermal evolution. Earth and Planetary Science Letters, 1999, 171, 63-81.	1.8	260
34	Trace Element Partitioning and Accessory Phase Saturation during H2O-Saturated Melting of Basalt with Implications for Subduction Zone Chemical Fluxes. Journal of Petrology, 2008, 49, 523-553.	1.1	260
35	Uranium–thorium disequilibria and partitioning on melting of garnet peridotite. Nature, 1993, 363, 63-65.	13.7	255
36	Systematics and energetics of trace-element partitioning between olivine and silicate melts: Implications for the nature of mineral/melt partitioning. Chemical Geology, 1994, 117, 57-71.	1.4	253

#	Article	IF	CITATIONS
37	Low-δ180 Rhyolites from Yellowstone: Magmatic Evolution Based on Analyses of Zircons and Individual Phenocrysts. Journal of Petrology, 2001, 42, 1491-1517.	1.1	252
38	An experimental study of trace element partitioning between zircon and melt as a function of oxygen fugacity. Geochimica Et Cosmochimica Acta, 2012, 95, 196-212.	1.6	244
39	REE fractionation and Nd-isotope disequilibrium during crustal anatexis: constraints from Himalayan leucogranites. Chemical Geology, 1997, 139, 249-269.	1.4	241
40	Magma Evolution and Open-System Processes at Shiveluch Volcano: Insights from Phenocryst Zoning. Journal of Petrology, 2006, 47, 2303-2334.	1.1	237
41	Li isotope fractionation in peridotites and mafic melts. Geochimica Et Cosmochimica Acta, 2007, 71, 202-218.	1.6	236
42	Partial melting and phase relations in high-grade metapelites: an experimental petrogenetic grid in the KFMASH system. Contributions To Mineralogy and Petrology, 1995, 120, 270-291.	1.2	235
43	Crystal-chemical controls on trace element partitioning between garnet and anhydrous silicate melt. American Mineralogist, 1999, 84, 838-847.	0.9	234
44	Kankan diamonds (Guinea) II: lower mantle inclusion parageneses. Contributions To Mineralogy and Petrology, 2000, 140, 16-27.	1.2	234
45	Zircon Tiny but Timely. Elements, 2007, 3, 13-18.	0.5	227
46	Primary carbonatite melt from deeply subducted oceanic crust. Nature, 2008, 454, 622-625.	13.7	225
47	The effect of Ca-Tschermaks component on trace element partitioning between clinopyroxene and silicate melt. Lithos, 2000, 53, 203-215.	0.6	224
48	Accessory phase controls on the geochemistry of crustal melts and restites produced during water-undersaturated partial melting. Contributions To Mineralogy and Petrology, 1993, 114, 550-566.	1.2	219
49	Partitioning of high field-strength and rare-earth elements between amphibole and quartz-dioritic to tonalitic melts: an experimental study. Chemical Geology, 1997, 138, 257-271.	1.4	219
50	SIMS analysis of oxygen isotopes: matrix effects in complex minerals and glasses. Chemical Geology, 1997, 138, 221-244.	1.4	211
51	Rapid decompression-driven crystallization recorded by melt inclusions from Mount St. Helens volcano. Geology, 2005, 33, 793.	2.0	207
52	Trace element distribution in annual stalagmite laminae mapped by micrometer-resolution X-ray fluorescence: Implications for incorporation of environmentally significant species. Geochimica Et Cosmochimica Acta, 2007, 71, 1494-1512.	1.6	205
53	Determination of partition coefficients between apatite, clinopyroxene, amphibole, and melt in natural spinel lherzolites from Yemen: Implications for wet melting of the lithospheric mantle. Geochimica Et Cosmochimica Acta, 1996, 60, 423-437.	1.6	200
54	A case for CO2-rich arc magmas. Earth and Planetary Science Letters, 2010, 290, 289-301.	1.8	198

#	Article	IF	CITATIONS
55	Experimental comparison of trace element partitioning between clinopyroxene and melt in carbonate and silicate systems, and implications for mantle metasomatism. Contributions To Mineralogy and Petrology, 2000, 139, 356-371.	1.2	197
56	Evaporite mineral assemblages in the nakhlite (martian) meteorites. Earth and Planetary Science Letters, 2000, 176, 267-279.	1.8	191
57	Sodium partitioning between clinopyroxene and silicate melts. Journal of Geophysical Research, 1995, 100, 15501-15515.	3.3	190
58	High-pressure Hydrous Phase Relations of Radiolarian Clay and Implications for the Involvement of Subducted Sediment in Arc Magmatism. Journal of Petrology, 2010, 51, 2211-2243.	1.1	190
59	Seasonal variations in Sr, Mg and P in modern speleothems (Grotta di Ernesto, Italy). Chemical Geology, 2001, 175, 429-448.	1.4	186
60	In situ U–Pb rutile dating by LA-ICP-MS: 208Pb correction and prospects for geological applications. Contributions To Mineralogy and Petrology, 2011, 162, 515-530.	1.2	186
61	Trace element partitioning on the Tinaquillo Lherzolite solidus at 1.5GPa. Physics of the Earth and Planetary Interiors, 2003, 139, 129-147.	0.7	185
62	Low-Temperature Carbonate Concretions in the Martian Meteorite ALH84001: Evidence from Stable Isotopes and Mineralogy. Science, 1997, 275, 1633-1638.	6.0	183
63	Silicon and Oxygen Self-Diffusivities in Silicate Liquids Measured to 15 Gigapascals and 2800 Kelvin. Science, 1997, 276, 1245-1248.	6.0	183
64	Aragonite-Calcite Relationships in Speleothems (Grotte De Clamouse, France): Environment, Fabrics, and Carbonate Geochemistry. Journal of Sedimentary Research, 2002, 72, 687-699.	0.8	182
65	Mineral-Melt Partitioning of Uranium, Thorium and Their Daughters. Reviews in Mineralogy and Geochemistry, 2003, 52, 59-123.	2.2	181
66	Metasomatic processes in lherzolitic and harzburgitic domains of diamondiferous lithospheric mantle: REE in garnets from xenoliths and inclusions in diamonds. Earth and Planetary Science Letters, 1998, 159, 1-12.	1.8	180
67	The trace element composition of silicate inclusions in diamonds: a review. Lithos, 2004, 77, 1-19.	0.6	180
68	Annual trace element variations in a Holocene speleothem. Earth and Planetary Science Letters, 1998, 154, 237-246.	1.8	179
69	Structure of the 8200-Year Cold Event Revealed by a Speleothem Trace Element Record. Science, 2002, 296, 2203-2206.	6.0	179
70	The generation of uranium series disequilibria by partial melting of spinel peridotite: constraints from partitioning studies. Earth and Planetary Science Letters, 1993, 117, 379-391.	1.8	178
71	Apatite: A new redox proxy for silicic magmas?. Geochimica Et Cosmochimica Acta, 2014, 132, 101-119.	1.6	178
72	Quantifying physiological influences on otolith microchemistry. Methods in Ecology and Evolution, 2015, 6, 806-816.	2.2	172

#	Article	IF	CITATIONS
73	Si and O diffusion in olivine and implications for characterizing plastic flow in the mantle. Geophysical Research Letters, 2002, 29, 26-1.	1.5	169
74	Development of microporosity, diffusion channels and deuteric coarsening in perthitic alkali feldspars. Contributions To Mineralogy and Petrology, 1990, 104, 507-515.	1.2	167
75	Diffusion of Li in olivine. Part I: Experimental observations and a multi species diffusion model. Geochimica Et Cosmochimica Acta, 2010, 74, 274-292.	1.6	167
76	Mineral inclusions in sublithospheric diamonds from Collier 4 kimberlite pipe, Juina, Brazil: subducted protoliths, carbonated melts and primary kimberlite magmatism. Contributions To Mineralogy and Petrology, 2010, 160, 489-510.	1.2	165
77	Silicate perovskite-melt partitioning of trace elements and geochemical signature of a deep perovskitic reservoir. Geochimica Et Cosmochimica Acta, 2005, 69, 485-496.	1.6	163
78	Correlated microanalysis of zircon: Trace element, δ18O, and U–Th–Pb isotopic constraints on the igneous origin of complex >3900Ma detrital grains. Geochimica Et Cosmochimica Acta, 2006, 70, 5601-5616.	1.6	158
79	Geochemistry of granitic melts produced during the incongruent melting of muscovite: Implications for the extraction of Himalayan leucogranite magmas. Journal of Geophysical Research, 1995, 100, 15767-15777.	3.3	156
80	The identification and significance of pure sediment-derived granites. Earth and Planetary Science Letters, 2017, 467, 57-63.	1.8	153
81	Boron and calcium isotope composition in Neoproterozoic carbonate rocks from Namibia: evidence for extreme environmental change. Earth and Planetary Science Letters, 2005, 231, 73-86.	1.8	152
82	Partitioning of F between H2O and CO2 fluids and topaz rhyolite melt. Contributions To Mineralogy and Petrology, 1990, 104, 424-438.	1.2	150
83	Plagioclase residence times at two island arc volcanoes (Kameni Islands, Santorini, and Soufriere, St.) Tj ETQq1 345-357.		rgBT /Overlo 149
84	Annual to sub-annual resolution of multiple trace-element trends in speleothems. Journal of the Geological Society, 2001, 158, 831-841.	0.9	148
85	Petrological cannibalism: the chemical and textural consequences of incremental magma body growth. Contributions To Mineralogy and Petrology, 2013, 166, 703-729.	1.2	148
86	Rare and unusual mineral inclusions in diamonds from Mwadui, Tanzania. Contributions To Mineralogy and Petrology, 1998, 132, 34-47.	1.2	147
87	Water solubility and chlorine partitioning in Cl-rich granitic systems: Effects of melt composition at 2 kbar and 800°C. Geochimica Et Cosmochimica Acta, 1992, 56, 679-687.	1.6	146
88	Metapelitic Migmatites from Brattstrand Bluffs, East Antarctica—Metamorphism, Melting and Exhumation of the Mid Crust. Journal of Petrology, 1996, 37, 395-414.	1.1	143
89	Reconstructing the deep CO2 degassing behaviour of large basaltic fissure eruptions. Earth and Planetary Science Letters, 2014, 393, 120-131.	1.8	143
90	lon microprobe trace-element analysis of silicates: Measurement of multi-element glasses. Chemical Geology, 1990, 83, 11-25.	1.4	142

#	Article	IF	CITATIONS
91	The impact of zircon–garnet REE distribution data on the interpretation of zircon U–Pb ages in complex high-grade terrains: An example from the Rauer Islands, East Antarctica. Chemical Geology, 2007, 241, 62-87.	1.4	141
92	The role of clinopyroxene in generating U-series disequilibrium during mantle melting. Geochimica Et Cosmochimica Acta, 1999, 63, 1613-1620.	1.6	139
93	Channelized Fluid Flow and Eclogite-facies Metasomatism along the Subduction Shear Zone. Journal of Petrology, 2014, 55, 883-916.	1.1	139
94	Near-solidus evolution of oceanic gabbros: insights from amphibole geochemistry. Geochimica Et Cosmochimica Acta, 2001, 65, 4339-4357.	1.6	138
95	The effect of cation charge on crystal–melt partitioning of trace elements. Earth and Planetary Science Letters, 2001, 188, 59-71.	1.8	138
96	Rates of hydrothermal cooling of new oceanic upper crust derived from lithium-geospeedometry. Earth and Planetary Science Letters, 2005, 240, 415-424.	1.8	137
97	Fluid-melt interactions involving Cl-rich granites: Experimental study from 2 to 8 kbar. Geochimica Et Cosmochimica Acta, 1992, 56, 659-678.	1.6	136
98	Magma Emplacement and Remobilization Timescales Beneath Montserrat: Insights from Sr and Ba Zonation in Plagioclase Phenocrysts. Journal of Petrology, 2003, 44, 1413-1431.	1.1	136
99	Experimental Simulation of Closed-System Degassing in the System Basalt–H2O–CO2–S–Cl. Journal of Petrology, 2011, 52, 1737-1762.	1.1	136
100	Experimental determination of the diffusion coefficient for calcium in olivine between 900°C and 1500°C. Geochimica Et Cosmochimica Acta, 2005, 69, 3683-3694.	1.6	134
101	High-temperature lithium isotope fractionation: Insights from lithium isotope diffusion in magmatic systems. Earth and Planetary Science Letters, 2007, 257, 609-621.	1.8	133
102	A matter of time: The importance of the duration of UHT metamorphism. Journal of Mineralogical and Petrological Sciences, 2016, 111, 50-72.	0.4	132
103	Melt geometry, movement and crystallization, in relation to mantle dykes, veins and metasomatism. Philosophical Transactions of the Royal Society: Physical and Engineering Sciences, 1993, 342, 1-21.	1.0	131
104	Kankan diamonds (Guinea) I: from the lithosphere down to the transition zone. Contributions To Mineralogy and Petrology, 2000, 140, 1-15.	1.2	131
105	Coralline algae are global palaeothermometers with bi-weekly resolution. Geochimica Et Cosmochimica Acta, 2008, 72, 771-779.	1.6	131
106	Concurrent Mixing and Cooling of Melts under Iceland. Journal of Petrology, 2008, 49, 1931-1953.	1.1	129
107	Cathodoluminescence and trace element zoning in quartz phenocrysts and xenocrysts. Geochimica Et Cosmochimica Acta, 1997, 61, 4337-4348.	1.6	128
108	Experimental determination of <scp>REE</scp> partition coefficients between zircon, garnet and melt: a key to understanding highâ€ <i>T</i> crustal processes. Journal of Metamorphic Geology, 2015, 33, 231-248.	1.6	128

#	Article	IF	CITATIONS
109	Ultrahigh temperature granulite metamorphism (1050 °C, 12 kbar) and decompression in garnet (Mg70)–orthopyroxene–sillimanite gneisses from the Rauer Group, East Antarctica. Journal of Metamorphic Geology, 1998, 16, 541-562.	1.6	126
110	Diamonds from the asthenosphere and the transition zone. European Journal of Mineralogy, 2001, 13, 883-892.	0.4	125
111	Evolving east Asian river systems reconstructed by trace element and Pb and Nd isotope variations in modern and ancient Red Riverâ€Song Hong sediments. Geochemistry, Geophysics, Geosystems, 2008, 9, .	1.0	125
112	Slow oxygen diffusion rates in igneous zircons from metamorphic rocks. American Mineralogist, 2003, 88, 1003-1014.	0.9	124
113	Partitioning of trace elements between clinopyroxene and garnet: data from mantle eclogites. Chemical Geology, 1997, 136, 1-24.	1.4	123
114	Cycling of B, Li, and LILE (K, Cs, Rb, Ba, Sr) into subduction zones: SIMS evidence from micas in high-P/T metasedimentary rocks. Chemical Geology, 2007, 239, 284-304.	1.4	123
115	Experimental partitioning of high field strength and rare earth elements between clinopyroxene and garnet in andesitic to tonalitic systems. Geochimica Et Cosmochimica Acta, 2000, 64, 99-115.	1.6	120
116	Atomistic simulation of trace element incorporation into garnets—comparison with experimental garnet-melt partitioning data. Geochimica Et Cosmochimica Acta, 2000, 64, 1629-1639.	1.6	118
117	Trace-element partitioning between apatite and carbonatite melt. American Mineralogist, 2003, 88, 639-646.	0.9	118
118	Zircon growth in UHT leucosome: constraints from zircon-garnet rare earth elements (REE) relations in Napier Complex, East Antarctica. Journal of Mineralogical and Petrological Sciences, 2004, 99, 180-190.	0.4	118
119	The impact of degassing on the oxidation state of basaltic magmas: A case study of Kīlauea volcano. Earth and Planetary Science Letters, 2016, 450, 317-325.	1.8	118
120	Abrupt global-ocean anoxia during the Late Ordovician–early Silurian detected using uranium isotopes of marine carbonates. Proceedings of the National Academy of Sciences of the United States of America, 2018, 115, 5896-5901.	3.3	118
121	Generation and preservation of continental crust in the Grenville Orogeny. Geoscience Frontiers, 2015, 6, 357-372.	4.3	117
122	Textural and chemical consequences of interaction between hydrous mafic and felsic magmas: an experimental study. Contributions To Mineralogy and Petrology, 2016, 171, 1.	1.2	117
123	Tracing Lithosphere Evolution through the Analysis of Heterogeneous G9-G10 Garnets in Peridotite Xenoliths, II: REE Chemistry. Journal of Petrology, 2004, 45, 609-633.	1.1	116
124	The causes and petrological significance of cathodoluminescence emissions from alkali feldspars. Contributions To Mineralogy and Petrology, 1999, 135, 234-243.	1.2	115
125	High field strength element/rare earth element fractionation during partial melting in the presence of garnet: Implications for identification of mantle heterogeneities. Geochemistry, Geophysics, Geosystems, 2001, 2, n/a-n/a.	1.0	114
126	Lead isotope variability in olivine-hosted melt inclusions from Iceland. Geochimica Et Cosmochimica Acta, 2008, 72, 4159-4176.	1.6	114

#	Article	IF	CITATIONS
127	The differentiation and rates of generation of the continental crust. Chemical Geology, 2006, 226, 134-143.	1.4	113
128	Annual trace element cycles in calcite-aragonite speleothems: evidence of drought in the western Mediterranean 1200-1100 yr BP. Journal of Quaternary Science, 2005, 20, 423-433.	1.1	110
129	Melt inclusions track pre-eruption storage and dehydration of magmas at Etna. Geology, 2009, 37, 571-574.	2.0	110
130	Late-stage volatile saturation as a potential trigger for explosive volcanic eruptions. Nature Geoscience, 2016, 9, 249-254.	5.4	110
131	Experimental investigations of the partitioning of Nb, Mo, Ba, Ce, Pb, Ra, Th, Pa, and U between immiscible carbonate and silicate liquids. Geochimica Et Cosmochimica Acta, 1995, 59, 1307-1320.	1.6	109
132	Trace element partitioning between mantle wedge peridotite and hydrous MgO-rich melt. American Mineralogist, 2003, 88, 1825-1831.	0.9	109
133	Diamond precipitation and mantle metasomatism - evidence from the trace element chemistry of silicate inclusions in diamonds from Akwatia, Ghana. Contributions To Mineralogy and Petrology, 1997, 129, 143-154.	1.2	107
134	The â€~zero charge' partitioning behaviour of noble gases during mantle melting. Nature, 2003, 423, 738-741.	13.7	107
135	The nature of erupting kimberlite melts. Lithos, 2009, 112, 429-438.	0.6	106
136	Ultra-Trace Element Analysis of NIST SRM 616 and 614 using Laser Ablation Microprobe-Inductively Coupled Plasma-Mass Spectrometry (LAM-ICP-MS): a Comparison with Secondary Ion Mass Spectrometry (SIMS). Geostandards and Geoanalytical Research, 1997, 21, 191-203.	1.7	105
137	Magma ascent rates in explosive eruptions: Constraints from H2O diffusion in melt inclusions. Earth and Planetary Science Letters, 2008, 270, 25-40.	1.8	105
138	Experimental Evidence for Polybaric Differentiation of Primitive Arc Basalt beneath St. Vincent, Lesser Antilles. Journal of Petrology, 2015, 56, 161-192.	1.1	104
139	Extreme crustal oxygen isotope signatures preserved in coesite in diamond. Nature, 2003, 423, 68-70.	13.7	102
140	The boron isotopic composition of tourmaline as a guide to fluid processes in the southwestern England orefield: An ion microprobe study. Geochimica Et Cosmochimica Acta, 1996, 60, 1415-1427.	1.6	100
141	Oxygen isotope evidence for slab-derived fluids in the sub-arc mantle. Nature, 1998, 393, 777-781.	13.7	100
142	Complexity in the behavior and recrystallization of monazite during high-T metamorphism and fluid infiltration. Chemical Geology, 2012, 322-323, 192-208.	1.4	100
143	lon microprobe analysis of oxygen isotope ratios in granulite facies magnetites: diffusive exchange as a guide to cooling history. Contributions To Mineralogy and Petrology, 1991, 109, 38-52.	1.2	99
144	Evidence from oceanic gabbros for porous melt migration within a crystal mush beneath the Mid-Atlantic Ridge. Geochemistry, Geophysics, Geosystems, 2000, 1, n/a-n/a.	1.0	99

#	Article	IF	CITATIONS
145	Geochemical Precursors to Volcanic Activity at Mount St. Helens, USA. Science, 2004, 306, 1167-1169.	6.0	99
146	Microchemical and Sr Isotopic Investigation of Zoned K-feldspar Megacrysts: Insights into the Petrogenesis of a Granitic System and Disequilibrium Crystal Growth. Journal of Petrology, 2005, 46, 1689-1724.	1.1	98
147	Do S-type granites commonly sample infracrustal sources? New results from an integrated O, U–Pb and Hf isotope study of zircon. Contributions To Mineralogy and Petrology, 2010, 160, 115-132.	1.2	98
148	Metasomatism of the shallow mantle beneath Yemen by the Afar plume—Implications for mantle plumes, flood volcanism, and intraplate volcanism. Geology, 1998, 26, 431.	2.0	97
149	Crystal–Melt Relationships and the Record of Deep Mixing and Crystallization in the ad 1783 Laki Eruption, Iceland. Journal of Petrology, 2013, 54, 1661-1690.	1.1	97
150	δ11B, Sr, Mg and B in a modern Porites coral: the relationship between calcification site pH and skeletal chemistry. Geochimica Et Cosmochimica Acta, 2010, 74, 1790-1800.	1.6	96
151	Linking granulites, silicic magmatism, and crustal growth in arcs: Ion microprobe (zircon) U-Pb ages from the Hidaka metamorphic belt, Japan. Geology, 2007, 35, 807.	2.0	95
152	Presalt stratigraphy and depositional systems in the Kwanza Basin, offshore Angola. AAPG Bulletin, 2016, 100, 1135-1164.	0.7	95
153	Carbon isotope ratios and nitrogen abundances in relation to cathodoluminescence characteristics for some diamonds from the Kaapvaal Province, S. Africa. Mineralogical Magazine, 1999, 63, 829-856.	0.6	94
154	Post-caldera volcanism: in situ measurement of U–Pb age and oxygen isotope ratio in Pleistocene zircons from Yellowstone caldera. Earth and Planetary Science Letters, 2001, 189, 197-206.	1.8	93
155	SIMS investigation of electron-beam damage to hydrous, rhyolitic glasses: Implications for melt inclusion analysis. American Mineralogist, 2006, 91, 667-679.	0.9	93
156	SIMS stable isotope measurement: counting statistics and analytical precision. Mineralogical Magazine, 2000, 64, 59-83.	0.6	92
157	Assimilation of Plutonic Roots, Formation of High-K â€ <sup></sup> Exotic' Melt Inclusions and Genesis of Andesitic Magmas at Volcán De Colima, Mexico. Journal of Petrology, 2008, 49, 2221-2243.	1.1	92
158	Palaeoenvironmental records from fossil corals: The effects of submarine diagenesis on temperature and climate estimates. Geochimica Et Cosmochimica Acta, 2007, 71, 4693-4703.	1.6	91
159	Corals concentrate dissolved inorganic carbon to facilitate calcification. Nature Communications, 2014, 5, 5741.	5.8	91
160	Exploring the plutonic-volcanic link: a zircon U-Pb, Lu-Hf and O isotope study of paired volcanic and granitic units from southeastern Australia. Transactions of the Royal Society of Edinburgh: Earth Sciences, 2008, 97, 337-355.	1.0	90
161	Sm-Nd isotopic evidence on the age of eclogitization in the Zermatt-Saas ophiolite. Journal of Metamorphic Geology, 1994, 12, 187-196.	1.6	88
162	U-series disequilibria generated by partial melting of spinel lherzolite. Earth and Planetary Science Letters, 2001, 188, 329-348.	1.8	88

#	Article	IF	CITATIONS
163	Clinopyroxene–melt trace element partitioning and the development of a predictive model for HFSE and Sc. Contributions To Mineralogy and Petrology, 2011, 161, 423-438.	1.2	88
164	Evidence for distinct stages of magma history recorded by the compositions of accessory apatite and zircon. Contributions To Mineralogy and Petrology, 2013, 166, 1-19.	1.2	88
165	The self-diffusion of silicon and oxygen in diopside (CaMgSi2O6) liquid up to 15 GPa. Chemical Geology, 2001, 174, 77-86.	1.4	87
166	Constraining the cooling rate of the lower oceanic crust: a new approach applied to the Oman ophiolite. Earth and Planetary Science Letters, 2002, 199, 127-146.	1.8	87
167	Origin of sub-lithospheric diamonds from the Juina-5 kimberlite (Brazil): constraints from carbon isotopes and inclusion compositions. Contributions To Mineralogy and Petrology, 2014, 168, 1.	1.2	87
168	A new tetragonal silicate mineral occurring as inclusions in lower-mantle diamonds. Nature, 1997, 387, 486-488.	13.7	86
169	Syngenetic inclusions in diamond from the Birim field (Ghana) - a deep peridotitic profile with a history of depletion and re-enrichment. Contributions To Mineralogy and Petrology, 1997, 127, 336-352.	1.2	86
170	Metasomatism and Partial Melting in Upper-Mantle Peridotite Xenoliths from the Lashaine Volcano, Northern Tanzania. Journal of Petrology, 2002, 43, 1749-1777.	1.1	86
171	A haliteâ€sideriteâ€anhydriteâ€chlorapatite assemblage in Nakhla: Mineralogical evidence for evaporites on Mars. Meteoritics and Planetary Science, 1999, 34, 407-415.	0.7	85
172	Effect of Fe2+ on garnet–melt trace element partitioning: experiments in FCMAS and quantification of crystal-chemical controls in natural systems. Lithos, 2000, 53, 189-201.	0.6	85
173	Oxygen isotope ratios of zircon: magma genesis of low δ18O granites from the British Tertiary Igneous Province, western Scotland. Earth and Planetary Science Letters, 2001, 184, 377-392.	1.8	85
174	In situ boron isotope analysis in marine carbonates and its application for foraminifera and palaeo-pH. Chemical Geology, 2009, 260, 138-147.	1.4	85
175	A geochemical and experimental study of the role of K-feldspar during water-undersaturated melting of metapelites. Chemical Geology, 1995, 122, 59-76.	1.4	84
176	lon microprobe analysis of oxygen isotope ratios in quartz from Skye granite: healed micro-cracks, fluid flow, and hydrothermal exchange. Contributions To Mineralogy and Petrology, 1996, 124, 225-234.	1.2	84
177	Experimental determination of aluminous clinopyroxene–melt partition coefficients for potassic liquids, with application to the evolution of the Roman province potassic magmas. Chemical Geology, 2001, 172, 213-223.	1.4	84
178	The continental lithospheric mantle: characteristics and significance as a mantle reservoir. Philosophical Transactions Series A, Mathematical, Physical, and Engineering Sciences, 2002, 360, 2383-2410.	1.6	83
179	Lithium Isotope Composition of Basalt Glass Reference Material. Analytical Chemistry, 2005, 77, 5251-5257.	3.2	82
180	Subduction, ophiolite genesis and collision history of Tethys adjacent to the Eurasian continental margin: new evidence from the Eastern Pontides, Turkey. Geodinamica Acta, 2013, 26, 230-293.	2.2	82

#	Article	IF	CITATIONS
181	Evidence for melting mud in Earth's mantle from extreme oxygen isotope signatures in zircon. Geology, 2017, 45, 975-978.	2.0	81
182	Compositional and temperature effects on sulfur speciation and solubility in silicate melts. Earth and Planetary Science Letters, 2019, 507, 187-198.	1.8	81
183	Variable water input controls evolution of the Lesser Antilles volcanic arc. Nature, 2020, 582, 525-529.	13.7	81
184	Cathodoluminescene at low Fe and Mn concentrations; a SIMS study of zones in natural calcites. Journal of Sedimentary Research, 1995, 65, 208-213.	0.8	80
185	Cosmogenic 3He concentrations in ancient flood deposits from the Coombs Hills, northern Dry Valleys, East Antarctica: interpreting exposure ages and erosion rates. Earth and Planetary Science Letters, 2005, 230, 163-175.	1.8	80
186	Compositional gaps in igneous rock suites controlled by magma system heat and water content. Nature Geoscience, 2013, 6, 385-390.	5.4	80
187	The effect of hydrogen on oxygen diffusion in quartz: evidence for fast proton transients?. Nature, 1988, 335, 243-245.	13.7	79
188	The effect of H2O on crystal-melt partitioning of trace elements. Geochimica Et Cosmochimica Acta, 2002, 66, 3647-3656.	1.6	79
189	Morphometry and composition of aragonite and vaterite otoliths of deformed laboratory reared juvenile herring from two populations. Journal of Fish Biology, 2003, 63, 1383-1401.	0.7	79
190	Hydrogen deficiency in Ti-rich biotite from anatectic metapelites (El Joyazo, SE Spain): Crystal-chemical aspects and implications for high-temperature petrogenesis. American Mineralogist, 2003, 88, 583-595.	0.9	79
191	Fractionation of Peralkaline Silicic Magmas: the Greater Olkaria Volcanic Complex, Kenya Rift Valley. Journal of Petrology, 2009, 50, 323-359.	1.1	79
192	Sedimentary recycling in arc magmas: geochemical and U–Pb–Hf–O constraints on the Mesoproterozoic Suldal Arc, SW Norway. Contributions To Mineralogy and Petrology, 2013, 165, 507-523.	1.2	79
193	Distribution of dissolved water in magmatic glass records growth and resorption of bubbles. Earth and Planetary Science Letters, 2014, 401, 1-11.	1.8	79
194	New constraints on electron-beam induced halogen migration in apatite. American Mineralogist, 2015, 100, 281-293.	0.9	79
195	Eclogitic and websteritic diamond sources beneath the Limpopo Belt – is slab-melting the link?. Contributions To Mineralogy and Petrology, 2002, 143, 56-70.	1.2	78
196	Trace elements and Li isotope systematics in Zabargad peridotites: evidence of ancient subduction processes in the Red Sea mantle. Chemical Geology, 2004, 212, 179-204.	1.4	78
197	Melting, Differentiation and Degassing at the Pantelleria Volcano, Italy. Journal of Petrology, 2012, 53, 637-663.	1.1	78
198	Giant magmatic water reservoirs at mid-crustal depth inferred from electrical conductivity and the growth of the continental crust. Earth and Planetary Science Letters, 2017, 457, 173-180.	1.8	78

#	Article	IF	CITATIONS
199	A predictive thermodynamic model of garnet–melt trace element partitioning. Contributions To Mineralogy and Petrology, 2001, 142, 219-234.	1.2	77
200	Melt percolation and reaction atop a plume: evidence from the poikiloblastic peridotite xenoliths from Borée (Massif Central, France). Contributions To Mineralogy and Petrology, 1998, 132, 65-84.	1.2	76
201	An investigation of closure temperature of the biotite Rb-Sr system: The importance of cation exchange. Geochimica Et Cosmochimica Acta, 2001, 65, 1141-1160.	1.6	76
202	Electrodeposition of Silicon from Nonaqueous Solvents. Journal of the Electrochemical Society, 2005, 152, C795.	1.3	76
203	The origin of Earth's first continents and the onset of plate tectonics. Geology, 2016, 44, 855-858.	2.0	76
204	Apatite trace element and isotope applications to petrogenesis and provenance. American Mineralogist, 2017, 102, 75-84.	0.9	76
205	Trace element distribution in Central Dabie eclogites. Contributions To Mineralogy and Petrology, 2000, 139, 298-315.	1.2	75
206	Multiple rhyolite magmas and basalt injection in the 17.7Âka Rerewhakaaitu eruption episode from Tarawera volcanic complex, New Zealand. Journal of Volcanology and Geothermal Research, 2007, 164, 1-26.	0.8	75
207	Chronology building using objective identification of annual signals in trace element profiles of stalagmites. Quaternary Geochronology, 2009, 4, 11-21.	0.6	75
208	Fe-XANES analyses of Reykjanes Ridge basalts: Implications for oceanic crust's role in the solid Earth oxygen cycle. Earth and Planetary Science Letters, 2015, 427, 272-285.	1.8	75
209	The volatile content of hypabyssal kimberlite magmas: some constraints from experiments on natural rock compositions. Bulletin of Volcanology, 2011, 73, 959-981.	1.1	74
210	Local variations of carbon isotope composition in diamonds from São-Luis (Brazil): Evidence for heterogenous carbon reservoir in sublithospheric mantle. Chemical Geology, 2014, 363, 114-124.	1.4	74
211	A predictive thermodynamic model for element partitioning between plagioclase and melt as a function of pressure, temperature and composition. Numerische Mathematik, 2014, 314, 1319-1372.	0.7	74
212	Silicate glasses in spinel lherzolites from Yemen: origin and chemical composition. Chemical Geology, 1996, 134, 159-179.	1.4	73
213	Calculated solution energies of heterovalent cations in forsterite and diopside: Implications for trace element partitioning. Geochimica Et Cosmochimica Acta, 1997, 61, 3927-3936.	1.6	73
214	Understanding the roles of crustal growth and preservation in the detrital zircon record. Earth and Planetary Science Letters, 2011, 305, 405-412.	1.8	73
215	Distribution of trace elements between amphibole and clinopyroxene from mantle peridotites of the Eifel (western Germany): An ion-microprobe study. Chemical Geology, 1994, 117, 235-250.	1.4	72
216	Chemical characteristics of migmatites: accessory phase distribution and evidence for fast melt segregation rates. Contributions To Mineralogy and Petrology, 1996, 125, 100-111.	1.2	72

#	Article	IF	CITATIONS
217	Trace-element content and partitioning in calcite, dolomite and apatite in carbonatite, Phalaborwa, South Africa. Mineralogical Magazine, 2003, 67, 921-930.	0.6	72
218	Tracking meteoric infiltration into a magmatic-hydrothermal system: A cathodoluminescence, oxygen isotope and trace element study of quartz from Mt. Leyshon, Australia. Chemical Geology, 2007, 240, 343-360.	1.4	72
219	Trace-element partitioning between garnet, clinopyroxene and Fe-rich picritic melts at 3 to 7ÂGPa. Contributions To Mineralogy and Petrology, 2007, 153, 369-387.	1.2	72
220	Fibrous diamonds from the placers of the northeastern Siberian Platform: carbonate and silicate crystallization media. Russian Geology and Geophysics, 2011, 52, 1298-1309.	0.3	72
221	Melt aggregation within the crust beneath the Mid-Atlantic Ridge: evidence from plagioclase and clinopyroxene major and trace element compositions. Earth and Planetary Science Letters, 2000, 176, 245-257.	1.8	71
222	Mineral inclusions in diamonds: associations and chemical distinctions around the 670-km discontinuity. Contributions To Mineralogy and Petrology, 2001, 142, 119-126.	1.2	71
223	The effect of sodium and titanium on crystal-melt partitioning of trace elements. Geochimica Et Cosmochimica Acta, 2004, 68, 2335-2347.	1.6	71
224	Millennial timescale resolution of rhyolite magma recharge at Tarawera volcano: insights from quartz chemistry and melt inclusions. Contributions To Mineralogy and Petrology, 2008, 156, 397-411.	1.2	71
225	Silicic recharge of multiple rhyolite magmas by basaltic intrusion during the 22.6Âka Okareka Eruption Episode, New Zealand. Lithos, 2008, 103, 527-549.	0.6	71
226	The 1874–1876 volcanoâ€ŧectonic episode at Askja, North Iceland: Lateral flow revisited. Geochemistry, Geophysics, Geosystems, 2013, 14, 2286-2309.	1.0	71
227	Eruption style at KÄ«lauea Volcano in Hawaiâ€~i linked to primary melt composition. Nature Geoscience, 2014, 7, 464-469.	5.4	71
228	Comparative determinations of trace and minor elements in coral aragonite by ion microprobe analysis, with preliminary results from Phuket, southern Thailand. Geochimica Et Cosmochimica Acta, 1996, 60, 3457-3470.	1.6	70
229	Mg in aragonitic bivalve shells: Seasonal variations and mode of incorporation in Arctica islandica. Chemical Geology, 2008, 254, 113-119.	1.4	70
230	Chlorine variations in the magma of Soufrière Hills Volcano, Montserrat: Insights from Cl in hornblende and melt inclusions. Geochimica Et Cosmochimica Acta, 2009, 73, 5693-5708.	1.6	70
231	Hydrous Phase Relations and Trace Element Partitioning Behaviour in Calcareous Sediments at Subduction-Zone Conditions. Journal of Petrology, 2015, 56, 953-980.	1.1	70
232	NIST SRM 610, 611 and SRM 612, 613 Multi-Element Glasses: Constraints from Element Abundance Ratios Measured by Microprobe Techniques. Geostandards and Geoanalytical Research, 1999, 23, 197-207.	1.7	69
233	Cordierite as a sensor of fluid conditions in high-grade metamorphism and crustal anatexis. Journal of Metamorphic Geology, 2002, 20, 71-86.	1.6	69
234	The evolution of a layered metaigneous complex in the Rauer Group, East Antarctica: evidence for a distinct Archaean terrane. Precambrian Research, 1998, 89, 175-205.	1.2	68

#	Article	IF	CITATIONS
235	The Nature of Young Vein Metasomatism in the Lithosphere of the West Eifel (Germany): Geochemical and Isotopic Constraints from Composite Mantle Xenoliths from the Meerfelder Maar. Journal of Petrology, 1998, 39, 155-185.	1.1	68
236	The Annandagstoppane Granite, East Antarctica: Evidence for Archaean Intracrustal Recycling in the Kaapvaal-Grunehogna Craton from Zircon O and Hf Isotopes. Journal of Petrology, 2010, 51, 2277-2301.	1.1	68
237	Ion-microprobe determinations of trace-element concentrations in garnets from anatectic assemblages. Chemical Geology, 1992, 100, 41-49.	1.4	67
238	An early Cambrian greenhouse climate. Science Advances, 2018, 4, eaar5690.	4.7	67
239	Pre-eruptive melt composition and constraints on degassing of a water-rich pantellerite magma, Fantale volcano, Ethiopia. Contributions To Mineralogy and Petrology, 1993, 114, 53-62.	1.2	66
240	Evidence for the multiple stage evolution of the subcontinental lithospheric mantle beneath the Eifel (Germany) from pyroxenite and composite pyroxenite/peridotite xenoliths. Contributions To Mineralogy and Petrology, 1998, 131, 258-272.	1.2	66
241	Accessory Mineral Behaviour in Granulite Migmatites: a Case Study from the Kerala Khondalite Belt, India. Journal of Petrology, 2014, 55, 1965-2002.	1.1	66
242	Volatile and lithophile trace-element geochemistry of Mexican tin rhyolite magmas deduced from melt inclusions. Geochimica Et Cosmochimica Acta, 1996, 60, 3267-3283.	1.6	65
243	Directional chemical variations in diamonds showing octahedral following cuboid growth. Contributions To Mineralogy and Petrology, 2006, 151, 45-57.	1.2	65
244	An apatite for progress: Inclusions in zircon and titanite constrain petrogenesis and provenance. Geology, 2016, 44, 91-94.	2.0	65
245	K-rich glass-bearing wehrlite xenoliths from Yitong, Northeastern China: petrological and chemical evidence for mantle metasomatism. Contributions To Mineralogy and Petrology, 1996, 125, 406-420.	1.2	64
246	Compositional effects on element partitioning between Mg-silicate perovskite and silicate melts. Contributions To Mineralogy and Petrology, 2005, 149, 113-128.	1.2	64
247	A snapshot of mantle metasomatism: Trace element analysis of coexisting fluid (LA-ICP-MS) and silicate (SIMS) inclusions in fibrous diamonds. Earth and Planetary Science Letters, 2009, 279, 362-372.	1.8	64
248	A Partial Record of Mixing of Mantle Melts Preserved in Icelandic Phenocrysts. Journal of Petrology, 2011, 52, 1791-1812.	1.1	64
249	Geodynamic controls on the contamination of Cenozoic arc magmas in the southern Central Andes: Insights from the O and Hf isotopic composition of zircon. Geochimica Et Cosmochimica Acta, 2015, 164, 386-402.	1.6	64
250	Listening In on the Past: What Can Otolith δ180 Values Really Tell Us about the Environmental History of Fishes?. PLoS ONE, 2014, 9, e108539.	1.1	64
251	Strontium heterogeneity and speciation in coral aragonite: implications for the strontium paleothermometer. Geochimica Et Cosmochimica Acta, 2001, 65, 2669-2676.	1.6	62
252	Vapor transfer prior to the October 2004 eruption of Mount St. Helens, Washington. Geology, 2007, 35, 231.	2.0	62

EIMF

#	Article	IF	CITATIONS
253	Trace element partitioning between orthopyroxene and anhydrous silicate melt on the lherzolite solidus from 1.1 to 3.2ÂGPa and 1,230 to 1,535°C in the model system Na2O–CaO–MgO–Al2O3–SiO2 Contributions To Mineralogy and Petrology, 2009, 157, 473-490.	.1.2	62
254	Development of crystallographic preferred orientation and microstructure during plastic deformation of natural coarseâ€grained quartz veins. Journal of Geophysical Research, 2010, 115, .	3.3	62
255	Two populations of carbonate in ALH84001: geochemical evidence for discrimination and genesis. Geochimica Et Cosmochimica Acta, 2002, 66, 1285-1303.	1.6	61
256	Extremely depleted lithospheric mantle and diamonds beneath the southern Zimbabwe Craton. Lithos, 2009, 112, 1120-1132.	0.6	61
257	Earthquakes as Precursors of Ductile Shear Zones in the Dry and Strong Lower Crust. Geochemistry, Geophysics, Geosystems, 2017, 18, 4356-4374.	1.0	61
258	Carbonatite Metasomatism of the Oceanic Upper Mantle: Evidence from Clinopyroxenes and Glasses in Ultramafic Xenoliths of Grande Comore, Indian Ocean. Journal of Petrology, 1999, 40, 133-165.	1.1	61
259	On the occurrence of apparent non-Henry's Law behaviour in experimental partitioning studies. Geochimica Et Cosmochimica Acta, 1993, 57, 47-55.	1.6	60
260	Regional-scale Grenvillian-age UHT metamorphism in the Mollendo-Camana block (basement of the) Tj ETQq0 0 0	rgBT /Ove	rlock 10 Tf
261	Textural and chemical variation in plagioclase phenocrysts from the 1980 eruptions of Mount St. Helens, USA. Contributions To Mineralogy and Petrology, 2007, 154, 291-308.	1.2	60
262	An Experimental Study of Trace Element Fluxes from Subducted Oceanic Crust. Journal of Petrology, 2015, 56, 1585-1606.	1.1	60
263	Formation and alteration of CAIs in Cold Bokkeveld (CM2). Geochimica Et Cosmochimica Acta, 1994, 58, 1913-1935.	1.6	59
264	Timescales and mechanisms of fluid infiltration in a marble: an ion microprobe study. Contributions To Mineralogy and Petrology, 1998, 132, 371-389.	1.2	59
265	Recent fluid processes in the Kaapvaal Craton, South Africa: coupled oxygen isotope and trace element disequilibrium in polymict peridotites. Earth and Planetary Science Letters, 2000, 176, 57-72.	1.8	59
266	Trace element variation in speleothem aragonite: potential for palaeoenvironmental reconstruction. Earth and Planetary Science Letters, 2001, 186, 255-267.	1.8	59
267	Anatexis during High-pressure Crustal Metamorphism: Evidence from Garnet–Whole-rock REE Relationships and Zircon–Rutile Ti–Zr Thermometry in Leucogranulites from the Bohemian Massif. Journal of Petrology, 2010, 51, 1967-2001.	1.1	59
268	Ar and K partitioning between clinopyroxene and silicate melt to 8 GPa. Geochimica Et Cosmochimica Acta, 2002, 66, 507-519.	1.6	58
269	Shallow-level decompression crystallisation and deep magma supply at Shiveluch Volcano. Contributions To Mineralogy and Petrology, 2007, 155, 45-61.	1.2	58

<sup>270</sup>High-resolution sulphur isotope analysis of speleothem carbonate by secondary ionisation mass<br/>spectrometry. Chemical Geology, 2010, 271, 101-107.1.458

#	Article	IF	CITATIONS
271	Petrogenesis and chronology of lunar meteorite Northwest Africa 4472: A KREEPy regolith breccia from the Moon. Geochimica Et Cosmochimica Acta, 2011, 75, 2420-2452.	1.6	58
272	Small volume andesite magmas and melt–mush interactions at Ruapehu, New Zealand: evidence from melt inclusions. Contributions To Mineralogy and Petrology, 2013, 166, 371-392.	1.2	58
273	Methods of laser-based stable isotope measurement applied to diagenetic cements and hydrocarbon reservoir quality. Clay Minerals, 2000, 35, 313-322.	0.2	57
274	Surviving mass extinction by bridging the benthic/planktic divide. Proceedings of the National Academy of Sciences of the United States of America, 2009, 106, 12629-12633.	3.3	57
275	Isovalent trace element partitioning between minerals and melts: A computer simulation study. Geochimica Et Cosmochimica Acta, 1996, 60, 4977-4987.	1.6	56
276	The Distribution of H2O between Cordierite and Granitic Melt: H2O Incorporation in Cordierite and its Application to High-grade Metamorphism and Crustal Anatexis. Journal of Petrology, 2001, 42, 1595-1620.	1.1	56
277	Ion microprobe analysis of 18O/16O in authigenic and detrital quartz in the St. Peter Sandstone, Michigan Basin and Wisconsin Arch, USA: Contrasting diagenetic histories. Geochimica Et Cosmochimica Acta, 1996, 60, 5101-5116.	1.6	55
278	Mg tracer diffusion in aluminosilicate garnets at 750-850°â€C, 1 atm. and 1300°â€C, 8.5 GPa. Contributior To Mineralogy and Petrology, 1996, 122, 406-414.	<sup>1S</sup> 1.2	55
279	Fractionation of lithium isotopes in magmatic systems as a natural consequence of cooling. Earth and Planetary Science Letters, 2009, 278, 286-296.	1.8	55
280	Tracking Volatile Behaviour in Sub-volcanic Plumbing Systems Using Apatite and Glass: Insights into Pre-eruptive Processes at Campi Flegrei, Italy. Journal of Petrology, 2018, 59, 2463-2492.	1.1	55
281	The nature of zircon inheritance in two granite plutons. Earth and Environmental Science Transactions of the Royal Society of Edinburgh, 1992, 83, 459-471.	0.3	54
282	Geochemical anomalies in coral skeletons and their possible implications for palaeoenvironmental analyses. Marine Chemistry, 1996, 55, 367-379.	0.9	54
283	Monazite behaviour and age significance in poly-metamorphic high-grade terrains: A case study from the western Musgrave Block, central Australia11Abbreviations: After Kretz, 1983 Lithos, 2006, 88, 100-134.	0.6	54
284	U and Th zonation in Fish Canyon Tuff zircons: Implications for a zircon (U–Th)/He standard. Geochimica Et Cosmochimica Acta, 2008, 72, 4745-4755.	1.6	54
285	Hydrogen incorporation and charge balance in natural zircon. Geochimica Et Cosmochimica Acta, 2014, 141, 472-486.	1.6	54
286	First recorded eruption of Nabro volcano, Eritrea, 2011. Bulletin of Volcanology, 2015, 77, 85.	1.1	54
287	Stable isotope evidence for crustal recycling as recorded by superdeep diamonds. Earth and Planetary Science Letters, 2015, 432, 374-380.	1.8	54
288	A novel mechanism for iron incorporation into coral skeletons. Coral Reefs, 1991, 10, 211-215.	0.9	53

#	Article	IF	CITATIONS
289	Rapid transcrustal magma movement under Iceland. Nature Geoscience, 2019, 12, 569-574.	5.4	53
290	Ion microprobe study of intragrain micropermeability in alkali feldspars. Contributions To Mineralogy and Petrology, 1990, 106, 124-128.	1.2	52
291	Extreme halogen abundances in tin-rich magma of the Taylor Creek Rhyolite, New Mexico. Economic Geology, 1994, 89, 840-850.	1.8	52
292	Uranium enrichment in metalliferous sediments from the Mid-Atlantic Ridge. Earth and Planetary Science Letters, 1994, 124, 35-47.	1.8	52
293	Self-diffusion in liquid Fe at high pressure. Physics of the Earth and Planetary Interiors, 2002, 130, 271-284.	0.7	52
294	Strontium in coral aragonite: 3. Sr coordination and geochemistry in relation to skeletal architecture. Geochimica Et Cosmochimica Acta, 2005, 69, 3801-3811.	1.6	52
295	A Temporal Record of Magma Accumulation and Evolution beneath Nevado de Toluca, Mexico, Preserved in Plagioclase Phenocrysts. Journal of Petrology, 2009, 50, 405-426.	1.1	52
296	Strontium distribution in the shell of the aragonite bivalve <i>Arctica islandica</i> . Geochemistry, Geophysics, Geosystems, 2009, 10, .	1.0	52
297	Magma storage conditions beneath Dabbahu Volcano (Ethiopia) constrained by petrology, seismicity and satellite geodesy. Bulletin of Volcanology, 2012, 74, 981-1004.	1.1	52
298	Extreme chemical variation in complex diamonds from George Creek, Colorado: a SIMS study of carbon isotope composition and nitrogen abundance. Mineralogical Magazine, 1999, 63, 857-878.	0.6	51
299	Volatile element (B, Cl, F) behaviour in the roof of an axial magma chamber from the East Pacific Rise. Earth and Planetary Science Letters, 2003, 213, 447-462.	1.8	51
300	Using trace element correlation patterns to decipher a sanidine crystal growth chronology: An example from Taapaca volcano, Central Andes. Journal of Volcanology and Geothermal Research, 2006, 156, 291-301.	0.8	51
301	RAPID COMMUNICATIONS Complex quartz growth histories in granite revealed by scanning cathodoluminescence techniques. Geological Magazine, 1997, 134, 549-552.	0.9	50
302	Mineral chemistry of a zircon-bearing, composite, veined and metasomatised upper-mantle peridotite xenolith from kimberlite. Contributions To Mineralogy and Petrology, 2001, 140, 720-733.	1.2	50
303	Magmatic Differentiation at an Island-arc Caldera: Okmok Volcano, Aleutian Islands, Alaska. Journal of Petrology, 2008, 49, 857-884.	1.1	50
304	Dynamics of cementation in response to oil charge: Evidence from a Cretaceous carbonate field, U.A.E Sedimentary Geology, 2010, 228, 246-254.	1.0	50
305	Cryptic Grain-Scale Heterogeneity of Oxygen Isotope Ratios in Metamorphic Magnetite. Science, 1993, 259, 1729-1733.	6.0	49
306	Magma storage, transport and degassing during the 2008–10 summit eruption at Kīlauea Volcano, Hawaiâ€ĩi. Geochimica Et Cosmochimica Acta, 2013, 123, 284-301.	1.6	49

#	Article	IF	CITATIONS
307	Diffusive over-hydration of olivine-hosted melt inclusions. Earth and Planetary Science Letters, 2015, 425, 168-178.	1.8	49
308	Halogen (F, Cl, Br, I) behaviour in subducting slabs: A study of lawsonite blueschists in western Turkey. Earth and Planetary Science Letters, 2016, 442, 133-142.	1.8	49
309	Cost-effective <sup>17</sup> O enrichment and NMR spectroscopy of mixed-metal terephthalate metal–organic frameworks. Chemical Science, 2018, 9, 850-859.	3.7	49
310	Generation of I-type granitic rocks by melting of heterogeneous lower crust. Geology, 2018, 46, 907-910.	2.0	49
311	Diamondiferous lithospheric roots along the western margin of the Kalahari Craton?the peridotitic inclusion suite in diamonds from Orapa and Jwaneng. Contributions To Mineralogy and Petrology, 2004, 147, 32-47.	1.2	48
312	Boron isotopes in tourmaline from the ca. 3.7–3.8Ga Isua supracrustal belt, Greenland: Sources for boron in Eoarchean continental crust and seawater. Geochimica Et Cosmochimica Acta, 2015, 163, 156-177.	1.6	48
313	Ion probe measurements of National Institute of Standards and Technology standard reference material SRM 610 glass, trace elements. Analyst, The, 1995, 120, 1315.	1.7	47
314	Olivine-hosted melt inclusions as an archive of redox heterogeneity in magmatic systems. Earth and Planetary Science Letters, 2017, 479, 192-205.	1.8	47
315	Experimental study of a Kiglapait marginal rock and implications for trace element partitioning in layered intrusions. Chemical Geology, 1997, 141, 73-92.	1.4	46
316	Recent remobilisation of shallow-level intrusions on Montserrat revealed by hydrogen isotope composition of amphiboles. Earth and Planetary Science Letters, 2001, 185, 285-297.	1.8	46
317	Orthopyroxene-Corundum in Mg-Al-rich Granulites from the Oygarden Islands, East Antarctica. Journal of Petrology, 2004, 45, 1481-1512.	1.1	46
318	Trace element partitioning between majoritic garnet and silicate melt at 25GPa. Physics of the Earth and Planetary Interiors, 2004, 143-144, 407-419.	0.7	46
319	The nature of the lithospheric mantle near the Tancheng-Lujiang fault, China: an integration of texture, chemistry and O-isotopes. Chemical Geology, 1996, 134, 67-81.	1.4	45
320	Graphite morphologies from the Borrowdale deposit (NW England, UK): Raman and SIMS data. Contributions To Mineralogy and Petrology, 2009, 158, 37-51.	1.2	45
321	Coupled Interactions between Volatile Activity and Fe Oxidation State during Arc Crustal Processes. Journal of Petrology, 2015, 56, 795-814.	1.1	45
322	Trace element partitioning and substitution mechanisms in calcium perovskites. Contributions To Mineralogy and Petrology, 2005, 149, 85-97.	1.2	44
323	A cryptic record of magma mixing in diorites revealed by high-precision SIMS oxygen isotope analysis of zircons. Earth and Planetary Science Letters, 2008, 269, 105-117.	1.8	43
324	lon microprobe assessment of the heterogeneity of Mg/Ca, Sr/Ca and Mn/Ca ratios in <i>Pecten maximus</i> and <i>Mytilus edulis</i> (bivalvia) shell calcite precipitated at constant temperature. Biogeosciences, 2009, 6, 1209-1227.	1.3	43

#	Article	IF	CITATIONS
325	Pre- and syn-eruptive degassing and crystallisation processes of the 2010 and 2006 eruptions of Merapi volcano, Indonesia. Contributions To Mineralogy and Petrology, 2014, 168, 1.	1.2	43
326	Formation and evolution of high-pressure leucogranulites: Experimental constraints and unresolved issues. Physics and Chemistry of the Earth, 1999, 24, 299-304.	0.6	42
327	Insights into silicic melt generation using plagioclase, quartz and melt inclusions from the caldera-forming Rotoiti eruption, Taupo volcanic zone, New Zealand. Contributions To Mineralogy and Petrology, 2010, 160, 951-971.	1.2	42
328	Oxygen isotope variability in conodonts: implications for reconstructing Palaeozoic palaeoclimates and palaeoceanography. Journal of the Geological Society, 2012, 169, 239-250.	0.9	42
329	Micron-scale coupled carbon isotope and nitrogen abundance variations in diamonds: Evidence for episodic diamond formation beneath the Siberian Craton. Geochimica Et Cosmochimica Acta, 2013, 100, 176-199.	1.6	42
330	Intermontane basins and bimodal volcanism at the onset of the Sveconorwegian Orogeny, southern Norway. Precambrian Research, 2014, 252, 107-118.	1.2	42
331	Magma mixing and high fountaining during the 1959 KÄ«lauea Iki eruption, Hawaiâ€~i. Earth and Planetary Science Letters, 2014, 400, 102-112.	1.8	42
332	Petrology and volatile content of magmas erupted from Tolbachik Volcano, Kamchatka, 2012–13. Journal of Volcanology and Geothermal Research, 2015, 307, 182-199.	0.8	42
333	Petrological and experimental evidence for differentiation of water-rich magmas beneath St. Kitts, Lesser Antilles. Contributions To Mineralogy and Petrology, 2017, 172, 98.	1.2	42
334	Effect of redox on Fe–Mg–Mn exchange between olivine and melt and an oxybarometer for basalts. Contributions To Mineralogy and Petrology, 2020, 175, 1.	1.2	42
335	Corroborated rainfall records from aragonitic stalagmites. Earth and Planetary Science Letters, 2003, 215, 265-273.	1.8	41
336	Mesoproterozoic subduction under the eastern edge of the Kalahari-Grunehogna Craton preceding Rodinia assembly: The Ritscherflya detrital zircon record, Ahlmannryggen (Dronning Maud Land,) Tj ETQq0 0 0 rgl	BT1/Øverlo	ck+10 Tf 50 2
337	Anticorrelation between low δ13C of eclogitic diamonds and high δ18O of their coesite and garnet inclusions requires a subduction origin. Geology, 2013, 41, 455-458.	2.0	41
338	Diamondiferous subcontinental lithospheric mantle of the northeastern Siberian Craton: Evidence from mineral inclusions in alluvial diamonds. Gondwana Research, 2015, 28, 106-120.	3.0	41
339	New SIMS U–Pb zircon ages from the Langavat Belt, South Harris, NW Scotland: implications for the Lewisian terrane model. Journal of the Geological Society, 2008, 165, 967-981.	0.9	40
340	Monitoring diamond crystal growth, a combined experimental and SIMS study. European Journal of Mineralogy, 2008, 20, 365-374.	0.4	40
341	Controls on Sr/Ca and Mg/Ca in scleractinian corals: The effects of Ca-ATPase and transcellular Ca channels on skeletal chemistry. Geochimica Et Cosmochimica Acta, 2011, 75, 6350-6360.	1.6	40
342	Monazite solubility in hydrous silicic melts at high pressure conditions relevant to subduction zone metamorphism. Earth and Planetary Science Letters, 2012, 321-322, 104-114.	1.8	40

#	Article	IF	CITATIONS
343	Lattice distortion in a zircon population and its effects on trace element mobility and U–Th–Pb isotope systematics: examples from the Lewisian Gneiss Complex, northwest Scotland. Contributions To Mineralogy and Petrology, 2013, 166, 21-41.	1.2	40
344	Silica burial enhanced by iron limitation in oceanic upwelling margins. Nature Geoscience, 2014, 7, 541-546.	5.4	40
345	Estimating the carbon content of the deep mantle with Icelandic melt inclusions. Earth and Planetary Science Letters, 2019, 523, 115699.	1.8	40
346	On the kinetics of textural equilibration in forsterite marbles. Contributions To Mineralogy and Petrology, 1991, 108, 356-367.	1.2	39
347	Volatile characteristics of peralkaline rhyolites from Kenya: an ion microprobe, infrared spectroscopic and hydrogen isotope study. Contributions To Mineralogy and Petrology, 1993, 114, 264-275.	1.2	39
348	Oxygen isotope diffusion and zoning in diopside: the importance of water fugacity during cooling. Geochimica Et Cosmochimica Acta, 1998, 62, 2265-2277.	1.6	39
349	Biological and ecological insights into Ca isotopes in planktic foraminifers as a palaeotemperature proxy. Earth and Planetary Science Letters, 2008, 271, 292-302.	1.8	39
350	Composition of cloudy microinclusions in octahedral diamonds from the Internatsional'naya kimberlite pipe (Yakutia). Russian Geology and Geophysics, 2011, 52, 85-96.	0.3	39
351	Eclogite formation beneath the northern Slave craton constrained by diamond inclusions: Oceanic lithosphere origin without a crustal signature. Earth and Planetary Science Letters, 2012, 319-320, 165-177.	1.8	39
352	Melt inclusion constraints on the magma source of Eyjafjallajökull 2010 flank eruption. Journal of Geophysical Research, 2012, 117, .	3.3	39
353	Eoarchaean tectonics: New constraints from high pressure-temperature experiments and mass balance modelling. Precambrian Research, 2019, 325, 20-38.	1.2	39
354	Contrasting styles of hydrous metasomatism in the upper mantle: An ion microprobe investigation. Geochimica Et Cosmochimica Acta, 1996, 60, 1367-1385.	1.6	38
355	Evidence of subduction and crust–mantle mixing from a single diamond. Lithos, 2004, 77, 349-358.	0.6	38
356	Volatiles contents, degassing and crystallisation of intermediate magmas at Volcan de Colima, Mexico, inferred from melt inclusions. Contributions To Mineralogy and Petrology, 2013, 165, 1087-1106.	1.2	38
357	Boron isotopic composition of tourmaline, prismatine, and grandidierite from granulite facies paragneisses in the Larsemann Hills, Prydz Bay, East Antarctica: Evidence for a non-marine evaporite source. Geochimica Et Cosmochimica Acta, 2013, 123, 261-283.	1.6	38
358	Merwinite in diamond from Sao Luiz, Brazil: A new mineral of the Ca-rich mantle environment. American Mineralogist, 2014, 99, 547-550.	0.9	38
359	The role of changing geodynamics in the progressive contamination of Late Cretaceous to Late Miocene arc magmas in the southern Central Andes. Lithos, 2016, 262, 169-191.	0.6	38
360	Extensive, water-rich magma reservoir beneath southern Montserrat. Lithos, 2016, 252-253, 216-233.	0.6	38

#	Article	IF	CITATIONS
361	Water transfer during magma mixing events: Insights into crystal mush rejuvenation and melt extraction processes. American Mineralogist, 2017, 102, 766-776.	0.9	38
362	Volatile and light lithophile elements in high-anorthite plagioclase-hosted melt inclusions from Iceland. Geochimica Et Cosmochimica Acta, 2017, 205, 100-118.	1.6	38
363	Petrology and geochemistry of the 2014–2015 Holuhraun eruption, central Iceland: compositional and mineralogical characteristics, temporal variability and magma storage. Contributions To Mineralogy and Petrology, 2018, 173, 1.	1.2	38
364	Natural experimental charges: an ion-microprobe study of trace element distribution coefficients in glass-rich hornblendite and clinopyroxenite xenoliths. Lithos, 2004, 75, 1-17.	0.6	37
365	The extent of U-series disequilibria produced during partial melting of the lower crust with implications for the formation of the Mount St. Helens dacites. Contributions To Mineralogy and Petrology, 2004, 148, 122-130.	1.2	37
366	Oxygen isotope sector zoning in natural hydrothermal quartz. Mineralogical Magazine, 2009, 73, 615-632.	0.6	37
367	Deep mixing of mantle melts beneath continental flood basalt provinces: Constraints from olivine-hosted melt inclusions in primitive magmas. Geochimica Et Cosmochimica Acta, 2017, 196, 36-57.	1.6	37
368	Phenocrystic fluorite in peralkaline rhyolites, Olkaria, Kenya Rift Valley. Mineralogical Magazine, 1998, 62, 477-486.	0.6	36
369	Cumulate clasts in the Bellecombe Ash Member, Piton de la Fournaise, Réunion Island, and their bearing on cumulative processes in the petrogenesis of the Réunion lavas. Journal of Volcanology and Geothermal Research, 2000, 104, 297-318.	0.8	36
370	Boron isotope and light element sector zoning in tourmaline: Implications for the formation of B-isotopic signatures. Chemical Geology, 2007, 238, 141-148.	1.4	36
371	Oxidised phase relations of a primitive basalt from Grenada, Lesser Antilles. Contributions To Mineralogy and Petrology, 2014, 167, 1.	1.2	36
372	The evolution and storage of primitive melts in the Eastern Volcanic Zone of Iceland: the 10Âka GrÃmsvötn tephra series (i.e. the Saksunarvatn ash). Contributions To Mineralogy and Petrology, 2015, 170, 1.	1.2	36
373	Assessing sulfur redox state and distribution in abyssal serpentinites using XANES spectroscopy. Earth and Planetary Science Letters, 2017, 466, 1-11.	1.8	36
374	Mantle garnets: A cracking yarn. Geochimica Et Cosmochimica Acta, 1992, 56, 2633-2642.	1.6	35
375	Cratonic peridotites and silica-rich melts: diopside-enstatite relationships in polymict xenoliths, Kaapvaal, South Africa. Geochimica Et Cosmochimica Acta, 2001, 65, 3365-3377.	1.6	35
376	Microscale variations of δ13C and N content within a natural diamond with mixed-habit growth. Chemical Geology, 2004, 205, 169-175.	1.4	35
377	Experimental and computational study of trace element distribution between orthopyroxene and anhydrous silicate melt: substitution mechanisms and the effect of iron. Contributions To Mineralogy and Petrology, 2010, 159, 459-473.	1.2	35
378	Temporal variations in the influence of the subducting slab on Central Andean arc magmas: Evidence from boron isotope systematics. Earth and Planetary Science Letters, 2014, 408, 390-401.	1.8	35

#	Article	IF	CITATIONS
379	Megacrystals track magma convection between reservoir and surface. Earth and Planetary Science Letters, 2015, 413, 1-12.	1.8	35
380	New evidence for Palaeoproterozoic high grade metamorphism in the Trivandrum Block, Southern India. Precambrian Research, 2016, 280, 120-138.	1.2	35
381	First measurements of OH-C exchange and temperature-dependent partitioning of OH and halogens in the system apatite–silicate melt. American Mineralogist, 2018, 103, 260-270.	0.9	35
382	The retrogradeP–T–tpath for lowâ€pressure granulites from the Reynolds Range, central Australia: petrological constraints and implications for lowâ€₽/highâ€Tmetamorphism. Journal of Metamorphic Geology, 1998, 16, 511-529.	1.6	34
383	Iron and water losses from hydrous basalts contained in Au80Pd20 capsules at high pressure and temperature. Mineralogical Magazine, 2004, 68, 75-81.	0.6	34
384	The role of TiO2 phases during melting of subduction-modified crust: Implications for deep mantle melting. Earth and Planetary Science Letters, 2008, 267, 301-308.	1.8	34
385	Lack of inhibiting effect of oil emplacement on quartz cementation: Evidence from Cambrian reservoir sandstones, Paleozoic Baltic Basin. Bulletin of the Geological Society of America, 2008, 120, 1280-1295.	1.6	34
386	Titanium- and water-rich metamorphic olivine in high-pressure serpentinites from the Voltri Massif (Ligurian Alps, Italy): evidence for deep subduction of high-field strength and fluid-mobile elements. Contributions To Mineralogy and Petrology, 2014, 167, 1.	1.2	34
387	Trace element composition of silicate inclusions in sub-lithospheric diamonds from the Juina-5 kimberlite: Evidence for diamond growth from slab melts. Lithos, 2016, 265, 108-124.	0.6	34
388	Pyroxenite and granulite xenoliths from beneath the Scottish Northern Highlands Terrane: evidence for lower-crust/upper-mantle relationships. Contributions To Mineralogy and Petrology, 2001, 142, 178-197.	1.2	33
389	Li abundances in inclusions in diamonds from the upper and lower mantle. Chemical Geology, 2003, 201, 307-318.	1.4	33
390	Trace element partitioning between baddeleyite and carbonatite melt at high pressures and high temperatures. Chemical Geology, 2003, 199, 233-242.	1.4	32
391	FTIR microspectroscopy and SIMS study of water-poor cordierite from El Hoyazo, Spain: Application to mineral and melt devolatilization. Lithos, 2009, 113, 498-506.	0.6	32
392	Alteration of soda silicate glasses by organic pollutants in museums: Mechanisms and kinetics. Journal of Non-Crystalline Solids, 2009, 355, 1479-1488.	1.5	32
393	Arc magma compositions controlled by linked thermal and chemical gradients above the subducting slab. Geophysical Research Letters, 2013, 40, 2550-2556.	1.5	32
394	An eclogitic diamond from Mir pipe (Yakutia), recording two growth events from different isotopic sources. Chemical Geology, 2014, 381, 40-54.	1.4	32
395	An experimental study of the behaviour of cerium/molybdenum ratios during subduction: Implications for tracing the slab component in the Lesser Antilles and Mariana Arc. Geochimica Et Cosmochimica Acta, 2017, 212, 133-155.	1.6	32
396	Melt inclusion constraints on volatile systematics and degassing history of the 2014–2015 Holuhraun eruption, Iceland. Contributions To Mineralogy and Petrology, 2018, 173, 1.	1.2	32

EIMF

#	Article	IF	CITATIONS
397	Crystal scavenging from mush piles recorded by melt inclusions. Nature Communications, 2019, 10, 5797.	5.8	32
398	Isotopic Compositions (Liâ€Bâ€Siâ€Oâ€Mgâ€Srâ€Ndâ€Hfâ€Pb) and Fe <sup>2+</sup> /ΣFe Ratios of Three Synt Glass Reference Materials (ARMâ€1, ARMâ€2, ARMâ€3). Geostandards and Geoanalytical Research, 2021, 45, 719-745.	hetic And 1.7	esite 32
399	Ion microprobe evidence for the mechanisms of stable isotope retrogression in high-grade metamorphic rocks. Contributions To Mineralogy and Petrology, 1995, 118, 365-378.	1.2	31
400	Geochemistry of mafic and ultramafic xenoliths from Fidra (Southern Uplands, Scotland): implications for lithospheric processes in Permo-Carboniferous times. Lithos, 2001, 58, 105-124.	0.6	31
401	Variations in Melt Productivity and Melting Conditions along SWIR (70°E–49°E): Evidence from Olivine-hosted and Plagioclase-hosted Melt Inclusions. Journal of Petrology, 2007, 48, 1471-1494.	1.1	31
402	Comparison of secondary ion mass spectrometry and micromilling/continuous flow isotope ratio mass spectrometry techniques used to acquire intraâ€otolith <i>í´</i> <sup>18</sup> 0 values of wild Atlantic salmon ( <i>Salmo salar</i> ). Rapid Communications in Mass Spectrometry, 2010, 24, 2491-2498.	0.7	31
403	Melt mixing causes negative correlation of trace element enrichment and CO2 content prior to an Icelandic eruption. Earth and Planetary Science Letters, 2014, 400, 272-283.	1.8	31
404	Diamond formation during metasomatism of mantle eclogite by chloride-carbonate melt. Contributions To Mineralogy and Petrology, 2018, 173, 1.	1.2	31
405	Reconstructing Magma Storage Depths for the 2018 KıÌ,,lauean Eruption From Melt Inclusion CO <sub>2</sub> Contents: The Importance of Vapor Bubbles. Geochemistry, Geophysics, Geosystems, 2021, 22, e2020GC009364.	1.0	31
406	Sapphirine granulites from the Vestfold Hills, East Antarctica: geochemical and metamorphic evolution. Antarctic Science, 1993, 5, 389-402.	0.5	30
407	Chevkinite-group minerals from salic volcanic rocks of the East African Rift. Mineralogical Magazine, 2002, 66, 287-299.	0.6	30
408	Pb isotopic variability in the modern-Pleistocene Indus River system measured by ion microprobe in detrital K-feldspar grains. Geochimica Et Cosmochimica Acta, 2011, 75, 4771-4795.	1.6	30
409	Evaluation of the effects of composition on instrumental mass fractionation during SIMS oxygen isotope analyses of glasses. Chemical Geology, 2012, 334, 312-323.	1.4	30
410	Chapter 16 Pre-eruptive vapour and its role in controlling eruption style and longevity at Soufrière Hills Volcano. Geological Society Memoir, 2014, 39, 291-315.	0.9	30
411	Trace Element Constraints on the Differentiation and Crystal Mush Solidification in the Skaergaard Intrusion, Greenland. Journal of Petrology, 2018, 59, 387-418.	1.1	30
412	The effect of melt composition and oxygen fugacity on manganese partitioning between apatite and silicate melt. Chemical Geology, 2019, 506, 162-174.	1.4	30
413	The evolution of the deep flow regime at Soultz-sous-Forêts, Rhine Graben, eastern France: Evidence from a composite quartz vein. Journal of Geophysical Research, 1998, 103, 27223-27237.	3.3	29
414	Computer simulation of high-temperature, forsterite-melt partitioning. American Mineralogist, 2000, 85, 1087-1091.	0.9	29

#	Article	IF	CITATIONS
415	Explosive subglacial rhyolitic eruptions in Iceland are fuelled by high magmatic H2O and closed-system degassing. Geology, 2013, 41, 251-254.	2.0	29
416	Petrological imaging of an active pluton beneath Cerro Uturuncu, Bolivia. Contributions To Mineralogy and Petrology, 2014, 167, 1.	1.2	29
417	Origin of Basalts by Hybridization in Andesite-dominated Arcs. Journal of Petrology, 2015, 56, 325-346.	1.1	29
418	The Late Cryogenian Warm Interval, NE Svalbard: Chemostratigraphy and genesis. Precambrian Research, 2016, 281, 128-154.	1.2	29
419	Syngenetic inclusions of yimengite in diamond from Sese kimberlite (Zimbabwe) — evidence for metasomatic conditions of growth. Lithos, 2004, 77, 181-192.	0.6	28
420	Crustal CO2 contribution to subduction zone degassing recorded through calc-silicate xenoliths in arc lavas. Scientific Reports, 2019, 9, 8803.	1.6	28
421	High fluxes of deep volatiles from ocean island volcanoes: Insights from El Hierro, Canary Islands. Geochimica Et Cosmochimica Acta, 2019, 258, 19-36.	1.6	28
422	Oxygen isotopes in titanite and apatite, and their potential for crustal evolution research. Geochimica Et Cosmochimica Acta, 2019, 255, 144-162.	1.6	28
423	A re-examination of the role of hydrogen in Alâ~'Si interdiffusion in feldspars. Contributions To Mineralogy and Petrology, 1990, 104, 481-491.	1.2	27
424	Surface chemistry of reacted heulandite determined by SIMS and XPS. Chemical Geology, 1996, 131, 167-181.	1.4	27
425	57Fe and Co tracer diffusion in liquid Fe–FeS at 2 and 5 GPa. Physics of the Earth and Planetary Interiors, 2000, 120, 137-144.	0.7	27
426	Pore water evolution in oilfield sandstones: constraints from oxygen isotope microanalyses of quartz cement. Chemical Geology, 2002, 191, 285-304.	1.4	27
427	The potential origins and palaeoenvironmental implications of high temporal resolution δ180 heterogeneity in coral skeletons. Geochimica Et Cosmochimica Acta, 2010, 74, 5537-5548.	1.6	27
428	Tectonic significance of Late Ordovician granitic magmatism and clastic sedimentation on the northern margin of Gondwana (Tavşanlű Zone, NW Turkey). Journal of the Geological Society, 2013, 170, 159-173.	0.9	27
429	pH up-regulation as a potential mechanism for the cold-water coral <i>Lophelia pertusa</i> to sustain growth in aragonite undersaturated conditions. Biogeosciences, 2015, 12, 6869-6880.	1.3	27
430	Geology and mineralogy of the Ashram Zone carbonatite, Eldor Complex, Québec. Ore Geology Reviews, 2017, 86, 784-806.	1.1	27
431	Deep roots for mid-ocean-ridge volcanoes revealed by plagioclase-hosted melt inclusions. Nature, 2019, 572, 235-239.	13.7	27
432	The distribution of H2O–CO2 between cordierite and granitic melt under fluid-saturated conditions at 5Âkbar and 900°C. Contributions To Mineralogy and Petrology, 2001, 142, 107-118.	1.2	26

#	Article	IF	CITATIONS
433	Combined C isotope and geochemical evidence for a recycled origin for diamondiferous eclogite xenoliths from kimberlites of Yakutia. Lithos, 2009, 112, 1032-1042.	0.6	26
434	Diffusion in diamond. I. Carbon isotope mapping of natural diamond. Mineralogical Magazine, 2009, 73, 193-200.	0.6	26
435	Experimental phase equilibria of a Mount St. Helens rhyodacite: a framework for interpreting crystallization paths in degassing silicic magmas. Contributions To Mineralogy and Petrology, 2015, 170, 1.	1.2	26
436	Volatileâ€Rich Magmas Distributed Through the Upper Crust in the Main Ethiopian Rift. Geochemistry, Geophysics, Geosystems, 2020, 21, e2019GC008904.	1.0	26
437	Megacrysts and Associated Xenoliths: Evidence for Migration of Geochemically Enriched Melts in the Upper Mantle beneath Scotland. , 0, .		26
438	An experimental replication of upper-mantle metasomatism. Nature, 1995, 373, 58-60.	13.7	25
439	The petrology of the Ditrau alkaline complex, Eastern Carpathians. Mineralogy and Petrology, 2000, 69, 227-265.	0.4	25
440	Petrology, mineralogy and geochemistry of oxide minerals in polymict xenoliths from the Bultfontein kimberlites, South Africa: implication for low bulk-rock oxygen isotopic ratios. Contributions To Mineralogy and Petrology, 2001, 141, 367-379.	1.2	25
441	Chapter 3.2 Ancient Antarctica: The Archaean of the East Antarctic Shield. Neoproterozoic-Cambrian Tectonics, Global Change and Evolution: A Focus on South Western Gondwana, 2007, 15, 149-186.	0.2	25
442	Carbon isotopes and nitrogen contents in placer diamonds from the NE Siberian craton: implications for diamond origins. European Journal of Mineralogy, 2014, 26, 41-52.	0.4	25
443	Mid-Miocene record of large-scale Snake River–type explosive volcanism and associated subsidence on the Yellowstone hotspot track: The Cassia Formation of Idaho, USA. Bulletin of the Geological Society of America, 2016, 128, 1121-1146.	1.6	25
444	Cathodoluminescence and microporosity in alkali feldspars from the BlÃ¥ MÃ¥ne SÃ, perthosite, South Greenland. Mineralogical Magazine, 1991, 55, 583-589.	0.6	24
445	Trace element partitioning between wollastonite and silicate-carbonate melt. Mineralogical Magazine, 2000, 64, 651-661.	0.6	24
446	Polycrystalline amphibole aggregates (clots) in granites as potential lâ€type restite: An ion microprobe study of rareâ€earth distributions. Australian Journal of Earth Sciences, 2001, 48, 591-601.	0.4	24
447	Atomistic simulations of trace element incorporation into the large site of MgSiO3 and CaSiO3 perovskites. Physics of the Earth and Planetary Interiors, 2003, 139, 113-127.	0.7	24
448	Corundum inclusions in diamonds—discriminatory criteria and a corundum compositional datasetâ~†. Lithos, 2004, 77, 273-286.	0.6	24
449	Growth medium composition of coated diamonds from the Sytykanskaya kimberlite pipe ( <i>Yakutia</i> ). Russian Geology and Geophysics, 2012, 53, 1197-1208.	0.3	24
450	Zr-in-rutile resetting in aluminosilicate bearing ultra-high temperature granulites: Refining the record of cooling and hydration in the Napier Complex, Antarctica. Lithos, 2017, 272-273, 128-146.	0.6	24

Еімғ

#	Article	IF	CITATIONS
451	Petrogenetic processes at the tipping point of plate tectonics: Hf-O isotope ternary modelling of Earth's last TTG to sanukitoid transition. Earth and Planetary Science Letters, 2020, 551, 116558.	1.8	24
452	The oxygen isotope anatomy of a slowly cooled metamorphic rock. American Mineralogist, 1995, 80, 757-764.	0.9	23
453	A Cool Early Earth?. Scientific American, 2005, 293, 58-65.	1.0	23
454	Reconstructing marine life-history strategies of wild Atlantic salmon from the stable isotope composition of otoliths. Marine Ecology - Progress Series, 2013, 475, 249-266.	0.9	23
455	Short Length Scale Oxygen Isotope Heterogeneity in the Icelandic Mantle: Evidence from Plagioclase Compositional Zones. Journal of Petrology, 2014, 55, 2537-2566.	1.1	23
456	Magmas Erupted during the Main Pulse of Siberian Traps Volcanism were Volatile-poor. Journal of Petrology, 2015, 56, 2089-2116.	1.1	23
457	Sulfur isotope signatures in the lower crust: A SIMS study on S-rich scapolite of granulites. Chemical Geology, 2017, 454, 54-66.	1.4	23
458	U–Pb isotopic dating of titanite microstructures: potential implications for the chronology and identification of large impact structures. Contributions To Mineralogy and Petrology, 2018, 173, 1.	1.2	23
459	Mixed mantle provenance: diverse garnet compositions in polymict peridotites, Kaapvaal craton, South Africa. Earth and Planetary Science Letters, 2003, 216, 329-346.	1.8	22
460	Trace metal (Mg/Ca and Sr/Ca) analyses of single coccoliths by Secondary Ion Mass Spectrometry. Geochimica Et Cosmochimica Acta, 2014, 146, 90-106.	1.6	22
461	Paleoecologic and paleoceanographic interpretation of δ180 variability in Lower Ordovician conodont species. Geology, 2018, 46, 467-470.	2.0	22
462	Textural and geochemical constraints on andesitic plug emplacement prior to the 2004–2010 vulcanian explosions at Galeras volcano, Colombia. Bulletin of Volcanology, 2019, 81, 1.	1.1	22
463	Experimental verification of the Stokes-Einstein relation in liquid Fe—FeS at 5 GPa. Molecular Physics, 2001, 99, 773-777.	0.8	21
464	Peridotitic diamonds from Namibia: constraints on the composition and evolution of their mantle source. Lithos, 2004, 77, 209-223.	0.6	21
465	Mineral inclusions in diamonds from the Kelsey Lake Mine, Colorado, USA: Depleted Archean mantle beneath the Proterozoic Yavapai province. Geochimica Et Cosmochimica Acta, 2008, 72, 1685-1695.	1.6	21
466	Identification and composition of secondary meniscus calcite in fossil coral and the effect on predicted sea surface temperature. Chemical Geology, 2011, 280, 314-322.	1.4	21
467	Temperature–time evolution of the Assynt Terrane of the Lewisian Gneiss Complex of Northwest Scotland from zircon U-Pb dating and Ti thermometry. Precambrian Research, 2015, 260, 55-75.	1.2	21
468	The 2011 eruption of Nabro volcano, Eritrea: perspectives on magmatic processes from melt inclusions. Contributions To Mineralogy and Petrology, 2018, 173, 1.	1.2	21

#	Article	IF	CITATIONS
469	Investigating ocean island mantle source heterogeneity with boron isotopes in melt inclusions. Earth and Planetary Science Letters, 2019, 508, 97-108.	1.8	21
470	Chemical diagenesis of carbonates in thin-sections: Ion microprobe as a trace element tool. Chemical Geology, 1987, 64, 225-237.	1.4	20
471	Determining pre-eruptive compositions of late Paleozoic magma from kaolinized volcanic ashes: Analysis of glass inclusions in quartz microphenocrysts from tonsteins. Geochimica Et Cosmochimica Acta, 1995, 59, 711-720.	1.6	20
472	Hidden melting signatures recorded in the Troodos ophiolite plutonic suite: evidence for widespread generation of depleted melts and intra-crustal melt aggregation. Contributions To Mineralogy and Petrology, 2003, 144, 484-506.	1.2	20
473	Statistical bias in isotope ratios. Journal of Analytical Atomic Spectrometry, 2013, 28, 52-58.	1.6	20
474	Understanding cold bias: Variable response of skeletal Sr/Ca to seawater pCO2 in acclimated massive Porites corals. Scientific Reports, 2016, 6, 26888.	1.6	20
475	Tectonic settings of continental crust formation: Insights from Pb isotopes in feldspar inclusions in zircon. Geology, 2016, 44, 819-822.	2.0	20
476	Electron microprobe technique for the determination of iron oxidation state in silicate glasses. American Mineralogist, 2018, 103, 1445-1454.	0.9	20
477	The effect of ocean acidification on tropical coral calcification: Insights from calcification fluid DIC chemistry. Chemical Geology, 2018, 497, 162-169.	1.4	20
478	Provenance and magmatic-tectonic setting of Campanian-aged volcaniclastic sandstones of the Kannaviou Formation in western Cyprus: Evidence for a South-Neotethyan continental margin volcanic arc. Sedimentary Geology, 2019, 388, 114-138.	1.0	20
479	Evidence from plutonic xenoliths for magma differentiation, mixing and storage in a volatile-rich crystal mush beneath St. Eustatius, Lesser Antilles. Contributions To Mineralogy and Petrology, 2019, 174, 39.	1.2	20
480	Boron isotope record of peak metamorphic ultrahigh-pressure and retrograde fluid–rock interaction in white mica (Lago di Cignana, Western Alps). Contributions To Mineralogy and Petrology, 2020, 175, 20.	1.2	20
481	Ion Microprobe Analysis of Oxygen, Carbon, and Hydrogen Isotope Ratios. , 1997, , 73-98.		20
482	Metamorphic olivine records external fluid infiltration during serpentinite dehydration. Geochemical Perspectives Letters, 0, 16, 25-29.	1.0	20
483	The implications of Sr-isotope disequilibrium for rates of prograde metamorphism and melt extraction in anatectic terrains. Geological Society Special Publication, 1998, 138, 171-182.	0.8	19
484	Iron Diffusion in Single-Crystal Diopside. Physics and Chemistry of Minerals, 2000, 27, 732-740.	0.3	19
485	A fertile harzburgite–garnet lherzolite transition: possible inferences for the roles of strain and metasomatism in upper mantle peridotites. Lithos, 2004, 77, 553-569.	0.6	19
486	Fast diffusion along mobile grain boundaries in calcite. Contributions To Mineralogy and Petrology, 2006, 153, 159-175.	1.2	19

Еімғ

#	Article	IF	CITATIONS
487	Deformation-controlled cation diffusion in tourmaline: A microanalytical study on trace elements and boron isotopes. American Mineralogist, 2007, 92, 1862-1874.	0.9	19
488	Degassing in kimberlite: Oxygen isotope ratios in perovskites from explosive and hypabyssal kimberlites. Earth and Planetary Science Letters, 2011, 312, 291-299.	1.8	19
489	Fluid inclusions in granulite-facies metapelites of the Hercynian ancient lower crust of the Serre, Calabria, Southern Italy. Contributions To Mineralogy and Petrology, 1992, 112, 393-404.	1.2	18
490	Ion microprobe study of oxygen isotopic compositions of structurally nonequivalent growth surfaces on synthetic calcite. Geochimica Et Cosmochimica Acta, 1997, 61, 5057-5063.	1.6	18
491	Ionic diffusion in quartz studied by transport measurements, SIMS and atomistic simulations. Journal of Physics Condensed Matter, 2005, 17, 1099-1112.	0.7	18
492	Trace element chemistry of mineral inclusions in eclogitic diamonds from the Premier (Cullinan) and Finsch kimberlites, South Africa: Implications for the evolution of their mantle source. Lithos, 2010, 118, 156-168.	0.6	18
493	Oxygen fugacity control in piston-cylinder experiments. Contributions To Mineralogy and Petrology, 2012, 164, 397-406.	1.2	18
494	Quantitative analysis of H2O and CO2 in cordierite using polarized FTIR spectroscopy. Contributions To Mineralogy and Petrology, 2012, 164, 881-894.	1.2	18
495	Using Zircon Isotope Compositions to Constrain Crustal Structure and Pluton Evolution: the Iapetus Suture Zone Granites in Northern Britain. Journal of Petrology, 2014, 55, 181-207.	1.1	18
496	A limited role for metasomatized subarc mantle in the generation of boron isotope signatures of arc volcanic rocks. Geology, 2019, 47, 517-521.	2.0	18
497	The role of sub-continental mantle as both "sink―and "source―in deep Earth volatile cycles. Geochimica Et Cosmochimica Acta, 2020, 275, 140-162.	1.6	18
498	The use of burial diagenetic calcite cements to determine the controls upon hydrocarbon emplacement and mineralization on a carbonate platform, Derbyshire, England. Geological Society Special Publication, 1996, 107, 35-49.	0.8	17
499	Major and trace element studies on garnets from Palaeozoic kimberlite-borne mantle xenoliths and megacrysts from the North China craton. Science in China Series D: Earth Sciences, 2000, 43, 423-430.	0.9	17
500	Sodium and potassium in cordierite a potential thermometer for melts?. European Journal of Mineralogy, 2002, 14, 459-469.	0.4	17
501	Two phases of sulphide saturation in Réunion magmas: Evidence from cumulates. Earth and Planetary Science Letters, 2012, 337-338, 104-113.	1.8	17
502	Melt inclusions in olivines from early Iceland plume picrites support high 3He/4He in both enriched and depleted mantle. Chemical Geology, 2012, 306-307, 54-62.	1.4	17
503	A combined geochronological approach to investigating long lived granite magmatism, the Shap granite, UK. Lithos, 2018, 304-307, 245-257.	0.6	17
504	Deep pre-eruptive storage of silicic magmas feeding Plinian and dome-forming eruptions of central and northern Dominica (Lesser Antilles) inferred from volatile contents of melt inclusions. Contributions To Mineralogy and Petrology, 2018, 173, 1.	1.2	17

#	Article	IF	CITATIONS
505	The role of sulfate-rich fluids in heavy rare earth enrichment at the Dashigou carbonatite deposit, Huanglongpu, China. Mineralogical Magazine, 2020, 84, 65-80.	0.6	17
506	The application of SIMS ion imaging techniques in the experimental study of fluid-mineral interactions. Mineralogical Magazine, 1991, 55, 347-356.	0.6	16
507	Diffusion in diamond. II. High-pressure-temperature experiments. Mineralogical Magazine, 2009, 73, 201-204.	0.6	16
508	The trace element geochemistry of clinopyroxenes from pyroxenites in the Lewisian of NW Scotland: insights into light rare earth element mobility during granulite facies metamorphism. Contributions To Mineralogy and Petrology, 2012, 163, 319-335.	1.2	16
509	Boron recycling in the mantle: Evidence from a global comparison of ocean island basalts. Geochimica Et Cosmochimica Acta, 2021, 302, 83-100.	1.6	16
510	Oxygen diffusion in sanidine feldspar and a critical appraisal of oxygen isotope-mass-effect measurements in non-cubic materials. Philosophical Magazine A: Physics of Condensed Matter, Structure, Defects and Mechanical Properties, 1997, 75, 485-503.	0.7	15
511	Petrogenesis of plagioclase phenocrysts of Mount Etna, Sicily, with particular reference to the 1983 eruption: contribution from cathodoluminescence petrography. Mineralogical Magazine, 1999, 63, 189-198.	0.6	15
512	Microstructural characterization of metamorphic magnetite crystals with implications for oxygen isotope distribution. American Mineralogist, 2000, 85, 14-21.	0.9	15
513	Sandstone cementation and fluids in hydrocarbon basins. Journal of Geochemical Exploration, 2000, 69-70, 195-200.	1.5	15
514	Oxygen isotope evidence for short-lived high-temperature fluid flow in the lower oceanic crust at fast-spreading ridges. Earth and Planetary Science Letters, 2007, 260, 524-536.	1.8	15
515	Effect of water on the fluorine and chlorine partitioning behavior between olivine and silicate melt. Contributions To Mineralogy and Petrology, 2017, 172, 15.	1.2	15
516	Detrital zircon age, oxygen and hafnium isotope systematics record rigid continents after 2.5†Ga. Gondwana Research, 2018, 57, 90-118.	3.0	15
517	Water-related defects and oxygen diffusion in albite: a computer simulation study. Contributions To Mineralogy and Petrology, 1996, 125, 161-166.	1.2	14
518	Isotopic Evolution of the Tonga Arc during Lau Basin Rifting; Evidence from the Volcaniclastic Record. Journal of Petrology, 1996, 37, 1153-1173.	1.1	14
519	Garnet pyroxenite xenoliths and pyropic megacrysts in Scottish alkali basalts. Scottish Journal of Geology, 2003, 39, 169-184.	0.1	14
520	Magma evolution beneath Bequia, Lesser Antilles, deduced from petrology of lavas and plutonic xenoliths. Contributions To Mineralogy and Petrology, 2018, 173, 1.	1.2	14
521	Mixing and Crystal Scavenging in the Main Ethiopian Rift Revealed by Trace Element Systematics in Feldspars and Glasses. Geochemistry, Geophysics, Geosystems, 2019, 20, 230-259.	1.0	14
522	Rapid pre-eruptive mush reorganisation and atmospheric volatile emissions from the 12.9 ka Laacher See eruption, determined using apatite. Earth and Planetary Science Letters, 2021, 576, 117198.	1.8	14

#	Article	IF	CITATIONS
523	Effects of seawater pH and calcification rate on test Mg/Ca and Sr/Ca in cultured individuals of the benthic, calcitic foraminifera Elphidium williamsoni. Chemical Geology, 2011, 289, 171-178.	1.4	13
524	A single-crystal neutron diffraction study of hambergite, Be2BO3(OH,F). American Mineralogist, 2012, 97, 1891-1897.	0.9	13
525	U–Pb dating constraints on the felsic and intermediate volcanic sequence of the nickel-sulphide bearing Cosmos succession, Agnew-Wiluna greenstone belt, Yilgarn Craton, Western Australia. Precambrian Research, 2013, 236, 85-105.	1.2	13
526	Oxygen isotopes in melt inclusions and glasses from the Askja volcanic system, North Iceland. Geochimica Et Cosmochimica Acta, 2013, 123, 55-73.	1.6	13
527	Detrital zircon U–Pb–Hf and O isotope character of the Cahill Formation and Nourlangie Schist, Pine Creek Orogen: Implications for the tectonic correlation and evolution of the North Australian Craton. Precambrian Research, 2014, 246, 35-53.	1.2	13
528	Primary aragonite and highâ€Mg calcite in the late Cambrian (Furongian). Potential evidence from marine carbonates in Oman. Terra Nova, 2016, 28, 306-315.	0.9	13
529	<sup>17</sup> O solid-state NMR spectroscopy of A <sub>2</sub> B <sub>2</sub> O <sub>7</sub> oxides: quantitative isotopic enrichment and spectral acquisition?. RSC Advances, 2018, 8, 7089-7101.	1.7	13
530	Constraints on the porosity, permeability and porous micro-structure of highly-crystalline andesitic magma during plug formation. Journal of Volcanology and Geothermal Research, 2019, 379, 72-89.	0.8	13
531	U-Pb geochronology of detrital and igneous zircon grains from the Ãguilas Arc in the Internal Betics (SE Spain): Implications for Carboniferous-Permian paleogeography of Pangea. Gondwana Research, 2021, 90, 135-158.	3.0	13
532	Deciphering variable mantle sources and hydrous inputs to arc magmas in Kamchatka. Earth and Planetary Science Letters, 2021, 562, 116848.	1.8	13
533	Biotites as Indicators of Fluorine Fugacities in Late-Stage Magmatic Fluids: the Gardar Province of South Greenland. Journal of Petrology, 1995, , .	1.1	12
534	Oxygen diffusion in anhydrous sanidine feldspar. Contributions To Mineralogy and Petrology, 1998, 133, 199-204.	1.2	12
535	Reconstructing Fluid Expulsion and Migration North of the Variscan Orogen, Northern England. Journal of Sedimentary Research, 2002, 72, 700-710.	0.8	12
536	The cordierite fluid monitor: case studies for and against its potential application. European Journal of Mineralogy, 2008, 20, 693-712.	0.4	12
537	Trace element geochemistry of nyerereite and gregoryite phenocrysts from natrocarbonatite lava, Oldoinyo Lengai, Tanzania: Implications for magma mixing. Lithos, 2012, 152, 56-65.	0.6	12
538	Zircon record of fractionation, hydrous partial melting and thermal gradients at different depths in oceanic crust (ODP Site 735B, South-West Indian Ocean). Contributions To Mineralogy and Petrology, 2017, 172, 1.	1.2	12
539	Trace-element geochemistry of diamond-hosted olivine inclusions from the Akwatia Mine, West African Craton: implications for diamond paragenesis and geothermobarometry. Contributions To Mineralogy and Petrology, 2019, 174, 1.	1.2	12
540	A SIMS U-Pb (zircon) and Re-Os (molybdenite) isotope study of the early Paleozoic Macquarie Arc, southeastern Australia: Implications for the tectono-magmatic evolution of the paleo-Pacific Gondwana margin. Gondwana Research, 2020, 82, 73-96.	3.0	12

#	Article	IF	Citations
541	Serial Mg/Ca and Sr/Ca chronologies across single benthic foraminifera tests. Chemical Geology, 2008, 253, 83-88.	1.4	11
542	A high resolution δ13C record in a modern Porites lobata coral: Insights into controls on skeletal δ13C. Geochimica Et Cosmochimica Acta, 2012, 84, 534-542.	1.6	11
543	Partitioning of light lithophile elements during basalt eruptions on Earth and application to Martian shergottites. Earth and Planetary Science Letters, 2015, 411, 142-150.	1.8	11
544	Syn-collisional detrital zircon source evolution in the northern Moroccan Variscides. Gondwana Research, 2021, 93, 73-88.	3.0	11
545	Ion Probe U-Pb Dating of the Central Sakarya Basement: A peri-Gondwana Terrane Intruded by Late Lower Carboniferous Subduction/Collision-related Granitic Rocks. Turkish Journal of Earth Sciences, 0, , .	0.4	11
546	The micro-/macro-diamond relationship: A case study from the Artemisia kimberlite (Northern Slave) Tj ETQqO O (	0 rgBT /O 9.6	verlock 10 Tf 5
547	Trace element thermometry of garnet-clinopyroxene pairs. American Mineralogist, 2016, 101, 1438-1450.	0.9	10
548	Experimental and Theoretical Evidence for Surface-Induced Carbon and Nitrogen Fractionation during Diamond Crystallization at High Temperatures and High Pressures. Crystals, 2017, 7, 190.	1.0	10
549	Step-like growth of the continental crust in South China: evidence from detrital zircons in Yangtze River sediments. Lithos, 2018, 320-321, 155-171.	0.6	10
550	The global melt inclusion C/Ba array: Mantle variability, melting process, or degassing?. Geochimica Et Cosmochimica Acta, 2021, 293, 525-543.	1.6	10
551	Boron isotopic signatures of melt inclusions from North Iceland reveal recycled material in the Icelandic mantle source. Geochimica Et Cosmochimica Acta, 2021, 294, 273-294.	1.6	10
552	Using zircon in mafic migmatites to disentangle complex high-grade gneiss terrains – Terrane spotting in the Lewisian complex, NW Scotland. Precambrian Research, 2021, 355, 106074.	1.2	10
553	Explosive Activity on KÄ«lauea's Lower East Rift Zone Fueled by a Volatileâ€Rich, Dacitic Melt. Geochemistry, Geophysics, Geosystems, 2022, 23, .	1.0	10
554	THE COMPOSITION OF ANORTHOCLASE AND NEPHELINE IN MOUNT KENYA PHONOLITE AND KILIMANJARO TRACHYTE, AND CRYSTAL-GLASS PARTITIONING OF ELEMENTS. Canadian Mineralogist, 2008, 46, 1455-1464.	0.3	9

555	The skeletal geochemistry of the sclerosponge Astrosclera willeyana: Implications for biomineralisation processes and palaeoenvironmental reconstruction. Palaeogeography, Palaeoclimatology, Palaeoecology, 2012, 313-314, 70-77.	1.0	9
556	Metasomatism and the crystallization of zircon megacrysts in Archaean peridotites from the Lewisian complex, NW Scotland. Contributions To Mineralogy and Petrology, 2018, 173, 99.	1.2	9
557	U–Pb detrital zircon ages used to infer provenance and tectonic setting of Late Triassic–Miocene sandstones related to the Tethyan development of Cyprus. Journal of the Geological Society, 2019, 176, 863-884.	0.9	9
558	Formation process of dunites and chromitites in Orhaneli and Harmancık ophiolites (NW Turkey): Evidence from in-situ Li isotopes and trace elements in olivine. Lithos, 2020, 376-377, 105773.	0.6	9

#	Article	IF	CITATIONS
559	Carbon isotope measurements on diamonds. Chemical Geology: Isotope Geoscience Section, 1992, 101, 177-183.	0.7	8
560	The anhydrous amphibole ungarettiite from the Woods mine, New South Wales, Australia. European Journal of Mineralogy, 2002, 14, 375-377.	0.4	8
561	Pre-eruptive volatile content, degassing paths and depressurisation explaining the transition in style at the subglacial rhyolitic eruption of DalakvÃsl, South Iceland. Journal of Volcanology and Geothermal Research, 2013, 258, 143-162.	0.8	8
562	The Eoarchaean foundation of the North Atlantic Craton. Geological Society Special Publication, 2015, 389, 261-279.	0.8	8
563	Matrix Effects During <scp>SIMS</scp> Measurement of the Lithium Mass Fractions of Silicate Glasses: Correction Procedures and Updated Preferred Values of Reference Materials. Geostandards and Geoanalytical Research, 2018, 42, 513-522.	1.7	8
564	An experimental investigation of F, Cl and H2O mineral-melt partitioning in a reduced, model lunar system. Geochimica Et Cosmochimica Acta, 2021, 294, 232-254.	1.6	8
565	DFENS: Diffusion Chronometry Using Finite Elements and Nested Sampling. Geochemistry, Geophysics, Geosystems, 2021, 22, e2020GC009303.	1.0	8
566	Influence of Deformation and Fluids on Ti Exchange in Natural Quartz. Journal of Geophysical Research: Solid Earth, 2021, 126, e2021JB022548.	1.4	8
567	Electron probe micro-analysis of oxygen in cordierite: potential implications for the analysis of volatiles in minerals. South African Journal of Geology, 2008, 111, 239-250.	0.6	7
568	Creep of mafic dykes infiltrated by melt in the lower continental crust (Seiland Igneous Province,) Tj ETQq0 0 0 rş	gBT /Overlo	əcķ 10 Tf 50 3
569	Experimental Simulations of Magma Storage and Ascent. Advances in Volcanology, 2017, , 101-110.	0.7	7
570	Evolution in magma storage conditions beneath Kick-'em-Jenny and Kick-'em-Jack submarine volcanoes, Lesser Antilles arc. Journal of Volcanology and Geothermal Research, 2019, 373, 1-22.	0.8	7
571	Micro-scale geochemical and crystallographic analysis of Buccinum undatum statoliths supports an annual periodicity of growth ring deposition. Chemical Geology, 2019, 526, 153-164.	1.4	7
572	Transcurrent displacement of the Cadomian magmatic arc. Precambrian Research, 2021, 361, 106251.	1.2	7
573	A Brilliant Future for Microanalysis?â€. Analyst, The, 1997, 122, 1187-1192.	1.7	6
574	The determination of partial melt compositions of peridotitic systems by melt inclusion synthesis. Contributions To Mineralogy and Petrology, 1997, 129, 209-221.	1.2	6

575	The Earth's deep interior: advances in theory and experiment. Philosophical Transactions Series A, Mathematical, Physical, and Engineering Sciences, 1999, 357, 3335-3357.	1.6	6
-----	---	-----	---

Carbon dioxide in pollucite, a feldspathoid with the ideal composition (Cs,) Tj ETQq0 0 0 rgBT /Overlock 10 Tf 50 67 Td (Na)<sub>16</sub>16</sub>16</sub>16</sub>16</sub>16</sub>16</sub>16</sub>16</sub>16</sub>16</sub>16</sub>16</sub>16</sub>16</sub>16</sub>16</sub>16</sub>16</sub>16</sub>16</sub>16</sub>16</sub>16</sub>16</sub>16</sub>16</sub>16</sub>16</sub>16</sub>16</sub>16</sub>16</sub>16</sub>16</sub>16</sub>16</sub>16</sub>16</sub>16</sub>16</sub>16</sub>16</sub>16</sub>16</sub>16</sub>16</sub>16</sub

#	Article	IF	CITATIONS
577	Taking the pulse of volcanic eruptions using plagioclase glomerocrysts. Earth and Planetary Science Letters, 2020, 552, 116596.	1.8	6
578	Instrumental mass fractionation during sulfur isotope analysis by secondary ion mass spectrometry in natural and synthetic glasses. Chemical Geology, 2021, 578, 120318.	1.4	6
579	Sulphur isotope analysis of pyrites. Chemical Geology: Isotope Geoscience Section, 1992, 101, 169-172.	0.7	5
580	Reservoir Sensitivity to Water Flooding: An Experimental Study of Seawater Injection in a North Sea Reservoir Analog. AAPG Bulletin, 1995, 79, .	0.7	5
581	Rare-earth-bearing minerals fergusonite and gadolinite from the Arran granite. Scottish Journal of Geology, 1999, 35, 65-69.	0.1	5
582	Deep and disturbed: conditions for formation and eruption of a mingled rhyolite at Ascension Island, south Atlantic. Volcanica, 2020, 3, 139-153.	0.6	5
583	Relative ion yields for SIMS analysis of trace elements in metallic Fe, Fe-Si alloy, and FeSi. International Journal of Mass Spectrometry, 2001, 207, 153-165.	0.7	4
584	SIMS sputtering rates in biogenic aragonite: implications for culture calibration studies for palaeoenvironmental reconstruction. Surface and Interface Analysis, 2013, 45, 1389-1394.	0.8	4
585	Reply to comment by Marks et al. (2016) on "Apatite: A new redox proxy for silicic magmas?― [Geochimica et Cosmochimica Acta 132 (2014) 101–119]. Geochimica Et Cosmochimica Acta, 2016, 183, 271-273.	1.6	4
586	Influences of coral genotype and seawater pCO2 on skeletal Ba/Ca and Mg/Ca in cultured massive Porites spp. corals. Palaeogeography, Palaeoclimatology, Palaeoecology, 2018, 505, 351-358.	1.0	4
587	The stability and composition of sulfate melts in arc magmas. Contributions To Mineralogy and Petrology, 2020, 175, 1.	1.2	4
588	Experimental evidence for decompression melting of metasomatized mantle beneath Colima Graben, Mexico. Contributions To Mineralogy and Petrology, 2020, 175, 1.	1.2	4
589	Early Miocene calc-alkaline felsic tuffs within deep-marine turbidites in the Kyrenia Range, north Cyprus, with a possible post-collisional eruptive centre in western Anatolia. Geological Magazine, 2021, 158, 1358-1370.	0.9	4
590	Strength of Dry and Wet Quartz in the Lowâ€Temperature Plasticity Regime: Insights From Nanoindentation. Geophysical Research Letters, 2022, 49, .	1.5	4
591	Oxygen isotope measurement of magnetites. Chemical Geology: Isotope Geoscience Section, 1992, 101, 173-176.	0.7	3
592	Textural and chemical zoning in garnets related to mantle metasomatism and deformation processes. Science Bulletin, 2000, 45, 174-180.	1.7	3
593	Mars-Analog Calcium Sulfate Veins Record Evidence of Ancient Subsurface Life. Astrobiology, 2020, 20, 1212-1223.	1.5	3
594	Formation of low-δ180 rhyolites after caldera collapse at Yellowstone, Wyoming, USA. Geology, 2000, 28, 719-722.	2.0	3

#	Article	IF	CITATIONS
595	K-poor titanian fluor-richterite from near Nullagine, Western Australia. American Mineralogist, 1995, 80, 162-164.	0.9	2
596	Discussion on â€~Magma storage region processes of the Soufrière Hills Volcano, Montserrat', Geological Society, London, Memoirs, 39, 361-381. Journal of the Geological Society, 2015, 172, 533-539.	0.9	2
597	Carbon Dioxide in Geochemically Heterogeneous Melt Inclusions From Mount Etna, Italy. Geochemistry, Geophysics, Geosystems, 2019, 20, 3150-3169.	1.0	2
598	Volcanic spherules condensed from supercritical fluids in the Payenia volcanic province, Argentina. Journal of the Geological Society, 2021, 178, .	0.9	2
599	The KD Sr/Ca in cultured massive Porites spp. corals are reduced at low seawater pCO2. Geochimica Et Cosmochimica Acta, 2021, 314, 55-67.	1.6	2
600	Cerchiaraite and Ca-bearing noelbensonite from Woods mine, New South Wales, Australia. European Journal of Mineralogy, 2004, 16, 185-189.	0.4	2
601	Insights Into the Nature of Plumeâ€Ridge Interaction and Outflux of H <sub>2</sub> O From the GalA¡pagos Spreading Center. Geochemistry, Geophysics, Geosystems, 2021, 22, e2020GC009560.	1.0	2
602	The influence of cordierite on melting and mineral-melt equilibria in ultra-high-temperature metamorphism. , 2004, , .		1
603	Evidence from Late Cretaceous-Paleogene volcanic rocks of the Kyrenia Range, northern Cyprus for the northern, active continental margin of the Southern Neotethys. Lithos, 2021, 380-381, 105835.	0.6	0
604	Ion Microprobe Imaging as a Tool for Elucidating Waterflood Reactions. AAPG Bulletin, 1996, 80, .	0.7	0